WL-TR-64-107

TR
WL
64-107

AD 609523

A LAGRANGIAN FINITE DIFFERENCE METHOD FOR TWO-DIMENSIONAL MOTION INCLUDING MATERIAL STRENGTH

by

Walter Herrmann
M. I. T.

AFWL TECHNICAL REPORT NO. WL-TR-64-107

16 6-p
COPY 2 OF 3 50
HARD COPY $. 3.00
MICROFICHE $. 0.75

Research and Technology Division
AIR FORCE WEAPONS LABORATORY
Air Force Systems Command
Kirtland Air Force Base
New Mexico

November 1964

DDC
RECEIVED
JAN 6 1965
DDC-IRA B

ARCHIVE COPY

Best
Available
Copy

Research and Technology Division
AIR FORCE WEAPONS LABORATORY
Air Force Systems Command
Kirtland Air Force Base
New Mexico

When U. S. Government drawings, specifications, or other data are used for any purpose other than a definitely related Government procurement operation, the Government thereby incurs no responsibility nor any obligation whatsoever, and the fact that the Government may have formulated, furnished, or in any way supplied the said drawings, specifications, or other data, is not to be regarded by implication or otherwise, as in any manner licensing the holder or any other person or corporation, or conveying any rights or permission to manufacture, use, or sell any patented invention that may in any way be related thereto.

This report is made available for study with the understanding that proprietary interests in and relating thereto will not be impaired. In case of apparent conflict or any other questions between the Government's rights and those of others, notify the Judge Advocate, Air Force Systems Command, Andrews Air Force Base, Washington, D. C. 20331.

DDC release to OTS is authorized.

WL-TR-64-107

A LAGRANGIAN FINITE DIFFERENCE METHOD FOR TWO-DIMENSIONAL MOTION INCLUDING MATERIAL STRENGTH

by

Walter Herrmann
M. I. T.

AFWL TECHNICAL REPORT NO. WL-TR-64-107

FOREWORD

This report was prepared by the Aeroelastic and Structures Research Laboratory, Department of Aeronautics and Astronautics, Massachusetts Institute of Technology. It is designated the Aeroelastic and Structures Research Laboratory Technical Report 106-2. The work reported was carried out under USAF Contract AF 29(601)-4601, Project 5776, Task 577601 and was administered by the Air Force Special Weapons Center, Kirtland Air Force Base, New Mexico. The inclusive dates for this research are 30 September 1962 through 24 June 1964.

This report was submitted by the author on 17 August 1964. AFWL Project Officer was Lt H. P. Ward, Jr., WLRPX.

The programming was carried out by Mrs. Evelyn Mack and Miss Margot O'Brien. The help of Miss Helen Petrides and the ASRL Computing Section is gratefully acknowledged.

This work was done in part at the Computation Center at the Massachusetts Institute of Technology, Cambridge, Massachusetts.

This research was funded by the Defense Atomic Support Agency under WEB No. 15.018.

This technical report has been reviewed and is approved.

H. P. WARD, JR.
Lt USAF
Project Officer

JOHN J. NEUER
Colonel USAF
Chief, Physics Branch

WILLIAM H. STEPHENS
Colonel USAF
Chief, Research Division

ABSTRACT

One- and two-space dimensional finite-difference schemes for the Lagrangian numerical solution of problems in the motion of solids, including material strength, are presented. Two-dimensional rectangular cartesian or cylindrically symmetric problems may be handled. Results of sample calculations are appended to illustrate the effect of material strength.

CONTENTS

Section		Page
I	INTRODUCTION	1
II	DIFFERENTIAL EQUATIONS	3
	2.1 Tensor Equations	3
	2.2 Two-Dimensional Equations in Physical Components	5
	2.3 One-Dimensional Equations in Physical Components	8
III	CONSTITUTIVE EQUATION	10
	3.1 Compressible Fluid	10
	3.2 Elastic Perfectly Plastic Material	12
	3.2.1 Tensor Equations	12
	3.2.2 Two-Dimensional Equations in Physical Components	15
	3.2.3 One-Dimensional Equations in Physical Components	18
	3.2.4 Geometrical Representation of Stress	20
IV	STABILITY	22
	4.1 Artificial Viscosity	22
	4.2 Stability Criterion	24
V	FINITE DIFFERENCE ANALOGS	26
VI	RESULTS	31
APPENDIX A	One-Dimensional Finite Difference Equations	36
	A.1 Equations of Motion	36
	A.2 Artificial Viscosity	38
	A.3 Fluid Constitutive Equation	39
	A.4 Elastic Perfectly Plastic Constitutive Equation	40
	A.5 High Explosive Constitutive Equation	43

		Page
	A.6 Energy Checks	45
	A.7 Boundary Conditions	48
	A.8 Stability Criterion	49
APPENDIX B	Two-Dimensional Finite Difference Equations	52
	B.1 Equations of Motion	52
	B.2 Continuity Equation	55
	B.3 Stretching and Spin	56
	B.4 Artificial Viscosity	57
	B.5 Stress Deviators	60
	B.6 Pressure	65
	B.7 Energy Checks	67
	B.8 Boundary Conditions	69
	B.9 Stability Criterion	71
APPENDIX C	Evaluation of Constitutive Equation Constants	73
	C.1 Solid or Fluid	74
	C.2 Nonideal Gas	79
REFERENCES		81
DISTRIBUTION		92

LIST OF FIGURES

Figure		Page
1	Elastic-Plastic Plate Impact at Initial Velocity 1.9 km/sec. Stress Profiles at 2 and 4 Microseconds	84
	Stress Profiles at 6 and 8 Microseconds	85
	Stress Profiles at 10 and 12 Microseconds	86
2	Fluid Plate Impact at Initial Velocity 1.9 km/sec. Stress Profiles at 2 and 4 Microseconds	87
	Stress Profiles at 6 and 8 Microseconds	88
	Stress Profiles at 10 and 12 Microseconds	89
3	Free Surface Velocity as a Function of Target Plate Thickness in Terms of Driver Plate Thickness for a Driver Plate Velocity of 1.9 km/sec.	90
4	Free Surface Velocity as a Function of Target Plate Thickness in Terms of Driver Plate Thickness for a Driver Plate Velocity of 1.2 km/sec.	91
5	Equation of State Schematic	92
6	Stress Profiles in an Aluminum Sphere Due to a Spherical Cavity Change of Pentolite	93
7	Cavity Radius vs. Time	94
8	Deformed Mesh Shapes for the Impact of an Aluminum Cylinder on a Smooth Wall	95
9	Stress Profiles for the Impact of an Aluminum Cylinder on a Smooth Wall	97

LIST OF SYMBOLS

a	Acceleration
c	Sound Speed
d	Stretching Tensor
f	Body Force
h	Heat Flux
k	Constants
p	Pressure
q	Viscous Stress
t	Stress; Time
u	Velocity
v	Volume
w	Spin
x, z	Coordinates
A	Area
B	Viscous Coefficient
G	Shear Modulus
K	Bulk Modulus
N	Unit Vectors
Q	Nonmechanical Energy
V	Volume
X, Z	Coordinate
Y	Yield Function

α	Symmetry Exponent
γ	Proportionality Constant
η	Compression
θ	Angle
λ, μ	Lame Constants
ν	Lode's Variable
ρ	Density
ϕ	Yield Function
ψ	Lode's Angle
$\mathcal{E}$	Internal Energy

SECTION I

INTRODUCTION

Solutions of problems in one- and two-dimensional (rectangular cartesian or cylindrically symmetric) fluid flow have been obtained by numerical integration using high speed digital computers. Such methods have been used widely to solve problems of dynamic deformation of solids due to high speed impact or due to detonation of high explosives. The assumption implicit in such an approach is that material strength may be neglected in comparison with the high pressures attending such motions.

Experimental evidence on craters resulting from very high velocity particle impact[1], and on the response of plates impacting at high velocity[2], indicates that material strength does influence the behaviour, even at high pressures and strain rates. An attempt has been made to incorporate material strength in a two-dimensional Lagrangian numerical integration scheme. During the course of this study, two similar studies were reported. The present work is essentially similar to that of Wilkins and Giroux[3] in most essential features. The scheme of Maenchen and Sack[4] is based on a different method of obtaining finite difference analogs.

The relevant differential equations have been

collected. These are developed into finite difference equations by the application of Green's Transformation. Results of a few sample calculations are included to demonstrate some of the qualitative effects of material strength.

SECTION II

DIFFERENTIAL EQUATIONS

2.1 Tensor Equations

The governing equations are the differential equations following from the principles of conservation of mass, momentum and energy.[5] From the principle of conservation of mass follows the continuity equation

$$\rho \, dv = \rho_o \, dV \qquad 2.1$$

where ρ is the density of the deformed volume element of material dv, and ρ_o the initial density of the undeformed volume element of material dV. The differential form of the continuity equation is also useful.

$$\dot{\rho} + \rho d^i_i = 0 \qquad 2.2$$

where the superimposed dot denotes the material derivative, and d^i_j is the stretching tensor defined by $d_{ij} = u_{(i,j)}$. Here $u^i = \dot{x}^i$ is the velocity and the comma denotes the covariant derivative.

The equation of motion follows from the principle of conservation of momentum

$$\rho a^k = \rho f^k + t^{(km)}{}_{,m}$$

$$t^{[km]} = 0 \qquad 2.3$$

where $a^k = \dot{u}^k$ is the acceleration, f^k the extrinsic (e.g. gravity) force and t^{km} is the (symmetric) stress tensor.

The principle of energy conservation and the definition of internal energy lead to the energy equation

$$\rho \dot{\varepsilon} = t^{km} d_{km} + h^k{}_{,k} + \rho Q \qquad 2.4$$

where ε is the internal energy per unit mass, h^k is the heat flux vector and Q the (chemical or other) energy supply per unit mass. It is more convenient to resolve the first term on the right, representing the stress work, into spherical and deviatoric parts. Writing

$$t^k_m = \frac{1}{3} t^i_i \delta^k_m + {}^d t^k_m \qquad 2.5$$

where the superscripted d denotes the deviator, and similarly for d^k_m, we have

$$t^{km} d_{km} = \frac{1}{3} t^i_i d^j_j + {}^d t^{km} {}^d d_{km} \qquad 2.6$$

Writing $p = -\frac{1}{3} t^i_i$ where p is the pressure, and using the differential form of the continuity equation, the energy equation takes the form

$$\rho \dot{\mathcal{E}} = p \frac{\dot{\rho}}{\rho} + {}^d t^{km} {}^d d_{km} + h^k{}_{,k} + Q \qquad 2.7$$

These equations are supplemented by the constitutive equation, describing the material behaviour, and the boundary conditions, which are described later.

2.2 Two-Dimensional Equations in Physical Components

The tensor equations are expanded in terms of physical components for rectangular and cylindrical polar coordinates for two independent space variables.

In two independent space variables, we consider rectangular symmetry, with no variation in quantities along the y axis, and cylindrical symmetry with no variation in quantities in the tangential, or θ direction. The physical equations

for both cases may be written down simultaneously by writing x and y in place of r and θ for the cylindrical polar case, and defining $\alpha = 1$ for rectangular, $\alpha = 2$ for cylindrical symmetry.

The equations of motion become

$$\left.\begin{aligned} \rho a^x &= \rho f^x + \frac{\partial t^{xx}}{\partial x} + \frac{\partial t^{xz}}{\partial z} + (\alpha - 1)\,\frac{t^{xx} - t^{yy}}{x} \\ \rho a^z &= \rho f^z + \frac{\partial t^{xz}}{\partial x} + \frac{\partial t^{zz}}{\partial z} + (\alpha - 1)\,\frac{t^{xz}}{x} \end{aligned}\right\} \quad 2.8$$

The velocity gradient $u_{i,j}$ has physical components

$$u_{a,b} = \begin{bmatrix} \frac{\partial u^x}{\partial x} & 0 & \frac{\partial u^x}{\partial z} \\ 0 & (\alpha - 1)\,\frac{u^x}{x} & 0 \\ \frac{\partial u^z}{\partial x} & 0 & \frac{\partial u^z}{\partial z} \end{bmatrix} \quad 2.9$$

where a , b take on successive values x , y , z and it is immaterial whether indices are written as subscripts or superscripts since the coordinates are orthogonal.

The differential form of the continuity equation becomes, directly

$$\dot{\rho} = -\rho \left\{ \frac{\partial u^x}{\partial x} + \frac{\partial u^z}{\partial z} + (\alpha - 1)\frac{u^x}{x} \right\} \qquad 2.10$$

In order to expand the energy equation we require the physical components of the stretching deviator

$$\left.\begin{aligned} {}^{d}d^{k}_{m} &= d^{k}_{m} - \frac{1}{3} d^{i}_{i} \delta^{k}_{m} \\ &= d^{k}_{m} + \frac{1}{3} \frac{\dot{\rho}}{\rho} \delta^{k}_{m} \end{aligned}\right\} \qquad 2.11$$

Thus we have physical components

$$ {}^{d}d_{(ab)} = \begin{bmatrix} \frac{\partial u^x}{\partial x} + \frac{1}{3}\frac{\dot{\rho}}{\rho} & 0 & \frac{1}{2}\left(\frac{\partial u^x}{\partial z} + \frac{\partial u^z}{\partial x}\right) \\ \cdot & (\alpha - 1)\frac{u^x}{x} + \frac{1}{3}\frac{\dot{\rho}}{\rho} & 0 \\ \cdot & \cdot & \frac{\partial u^z}{\partial z} + \frac{1}{3}\frac{\dot{\rho}}{\rho} \end{bmatrix} \qquad 2.12$$

and the energy equation becomes

$$\rho \frac{\partial \mathcal{E}}{\partial t} = p\frac{\dot{\rho}}{\rho} + \rho\, {}^{d}\dot{\mathcal{E}} + \left\{ \frac{\partial h^x}{\partial x} + \frac{\partial h^z}{\partial z} + (\alpha - 1)\frac{h^x}{x} \right\} + \rho Q \qquad 2.13$$

where the deviator stress work $\rho\, {}^{d}\dot{\mathcal{E}}$ may be written

$$\rho\, {}^{d}\dot{e} = 2\, {}^{d}t^{xx}\, {}^{d}d^{xx} + 2\, {}^{d}t^{xz}\, {}^{d}d^{xz} + 2\, {}^{d}t^{zz}\, {}^{d}d^{zz} + {}^{d}t^{xx}\, {}^{d}d^{zz} + {}^{d}t^{zz}\, {}^{d}d^{xx} \qquad 2.14$$

Since material particles will be followed in the computation, the velocities and accelerations are simply given by

$$u^{x} = \frac{\partial x}{\partial t} \qquad u^{z} = \frac{\partial z}{\partial t}$$

$$a^{x} = \frac{\partial u^{x}}{\partial t} \qquad a^{z} = \frac{\partial u^{z}}{\partial t} \qquad 2.15$$

2.3 One-Dimensional Equations in Physical Components

The tensor equations are expanded in terms of physical components for rectangular, cylindrical, and spherical polar coordinates with variation only in the x or radial direction. Proceeding similarly as in the two-dimensional case, further defining $\alpha = 3$ for spherical symmetry. Then the equation of motion reduces to

$$\rho a^{x} = \rho f^{x} + \frac{\partial t^{x}}{\partial x} + (\alpha - 1)\frac{t^{x} - t^{y}}{x} \qquad 2.16$$

There is no rotation, and the above stress components are principal components, which is expressed by use of a single superscript. Off-diagonal stretching components also disappear, and

$$d^{a} = \left[\frac{\partial u^{x}}{\partial x} \; ; \quad 0 \quad ; \quad 0 \right] \qquad \alpha = 1$$

$$d^{a} = \left[\frac{\partial u^{x}}{\partial x} \; ; \quad \frac{u^{x}}{x} \quad ; \quad 0 \right] \qquad \alpha = 2 \qquad 2.17$$

$$d^{a} = \left[\frac{\partial u^{x}}{\partial x} \; ; \quad \frac{u^{x}}{x} \quad ; \quad \frac{u^{x}}{x} \right] \qquad \alpha = 3$$

The energy equation reduces to

$$\rho \frac{\partial \mathcal{E}}{\partial t} = p \frac{\dot{\rho}}{\rho} + \rho^{d}\dot{\mathcal{E}} + \left\{ \frac{\partial h^{x}}{\partial x} + (\alpha - 1) \frac{h^{x}}{x} \right\} + \rho Q \qquad 2.18$$

where the deviator stress work is

$$\rho^{d}\dot{\mathcal{E}} = 2\,{}^{d}t^{x}\,{}^{d}d^{x} + 2\,{}^{d}t^{z}\,{}^{d}d^{z} + {}^{d}t^{x}\,{}^{d}d^{z} + {}^{d}t^{z}\,{}^{d}d^{x} \qquad 2.19$$

SECTION III

CONSTITUTIVE EQUATION

3.1 Compressible Fluid

We first discuss the constitutive equation of a fluid, which cannot support a shear stress while at rest. The total stress t^i_j entering the conservation equations may be expressed in terms of a thermodynamic (elastic) pressure ${}_e p$, a dissipative (viscous) pressure q, and a viscous stress deviator ${}^d q_j$

$$t^i_j = -({}_e p + q)\,\delta^i_j + {}^d q^i_j \qquad 3.1$$

The viscous stress tensor must be isotropic. Taking the viscous stress proportional to the stretchings, we have the following form

$$q^i_j = \lambda\, d^m_m\, \delta^i_j + 2\mu\, d^i_j \qquad 3.2$$

where λ and μ are here used as viscosity coefficients. Then

$$-q \equiv \frac{1}{3}\, q^m_m = \left(\lambda + \frac{2}{3}\mu\right) d^m_m \qquad 3.3$$

and for the deviator

$$ {}^{d}q^{i}_{j} = q^{i}_{j} + q\,\delta^{i}_{j} \qquad 3.4 $$

Using Equations 3.2 and 3.3 this reduces to

$$ {}^{d}q^{i}_{j} = 2\mu\,{}^{d}d^{i}_{j} \qquad 3.5 $$

where ${}^{d}d^{i}_{j}$ is the previously defined stretching deviator.

The viscosity coefficients may be "real" coefficients, representing the viscous behaviour of the material, if these can be evaluated. More usually artificial viscosity coefficients are used with specific properties to aid in maintaining stability of the finite difference calculation without unduly affecting the solution.[6] These will be discussed later.

The thermodynamic pressure ${}_{e}p$ is related to the thermodynamic state (ρ, $\mathcal{E}$). This relation will be taken in the form of power series in the compression $\eta = (\rho - \rho_0)/\rho$

$$ {}_{e}p = f_1(\rho) + \mathcal{E}\cdot f_2(\rho) $$

$$ f_1 = k_0\,\eta\left\{1 + k_1\eta + k_2\eta^2 + \cdots\right\} \qquad 3.6 $$

$$ f_2 = h_0\left\{1 + h_1\eta + h_2\eta^2 + \cdots\right\} $$

A similar equation of state is used for explosion product gases, but with different forms of the functions f_1 and f_2.

3.2 Elastic Perfectly Plastic Material

3.2.1 Tensor Equations

For a compressible material which is able to support a shear stress while at rest, it is necessary to add a non-dissipative (elastic) stress deviator to the previous expression for the total stress.

$$t^i_j = -({}_eP + q)\,\delta^i_j + ({}^d_e t^i_j + {}^d q^i_j) \qquad 3.7$$

The thermodynamic pressure and viscous stresses will be formulated as in the case of a fluid. Here we will consider the elastic stress deviator.

Making the usual assumptions of plasticity theory, modified to include large compressions,[7] viz:-

a) The stretching can be expressed as the sum of the elastic and plastic stretchings.

$$d^i_j = {}_e d^i_j + {}_p d^i_j \qquad 3.8$$

b) The spherical stretching (dilatation) is entirely elastic and recoverable, which is equivalent to assuming

$${}_p d^i_i = 0 \qquad 3.9$$

c) The elastic stress deviator is limited by the von Mises yield condition

$$\phi = \mathrm{II} - \frac{2}{3} Y^2 \leq 0 \qquad 3.10$$

where $\mathrm{II} = {}^{d}_{e}t^{i}_{j} \; {}^{d}_{e}t^{j}_{i}$ is the second moment of the stress deviator, and Y is a material constant. It is easily seen that Y is the yield stress in a uniaxial stress tensile test.

d) The plastic stretching is orthogonal to the yield surface, leading to the flow rule

$$ {}_{p}d^{i}_{j} = \zeta \frac{\partial \phi}{\partial {}_{e}t^{j}_{i}} \qquad 3.11$$

where ζ is an undetermined proportionality constant. For von Mises yield criterion, this reduces directly to

$$ {}_{p}d^{i}_{j} = \frac{\zeta}{\sqrt{\mathrm{II}}} \, {}^{d}_{e}t^{i}_{j} \qquad 3.12$$

In view of the fact that we have assumed ${}_{p}d^{i}_{i} = 0$, we may also write the stretching deviator on the left hand side of this equation.

e) The usual assumption of a linear relation between elastic stress rate and stretching must be modified to allow for finite compression. The usual assumption of an isotropic linear elastic medium is expressed in Hooke's Law

$$ \overset{\blacktriangledown}{t}{}^{i}_{j} = \lambda \, d^{m}_{m} \, \delta^{i}_{j} + 2\mu \, d^{i}_{j} \qquad 3.13$$

where λ and μ are now used as elasticity (Lamé) constants, and the superimposed triangle denotes objective stress rate. Resolving this expression into spherical and deviatoric parts as was done for the viscous stress tensor,

$$-\dot{p} = \left(\lambda + \frac{2}{3}\mu\right) d^i_i$$

3.14

$$\overset{\blacktriangledown}{{}^d t}{}^i_j = 2\mu \, {}^d d^i_j$$

We now make the special assumption that the elastic deviatoric strain, which is limited in effect by the yield condition, always remains small. We are then concerned only with small deviations from a hydrostatic state, and make the assumption that the material remains isotropic. We thus generalize the above equations by writing

$$-\dot{p} = -K \frac{\dot{\rho}}{\rho}$$

3.15

$$\overset{\blacktriangledown}{{}^d t}{}^i_j = 2G \, {}^d d^i_j$$

where K, the bulk modulus, and G, the shear modulus, are taken to be functions of the thermodynamic state $(\rho, \mathcal{E})$. It is of course more convenient to use the integrated version of Equation 3.15a, that is Equation 3.6, for the spherical part.

The equations necessary to determine the elastic stress deviator from the stretching deviator are therefore

$$ {}^{d}d^{i}_{j} = {}^{d}_{e}d^{i}_{j} + {}^{d}_{p}d^{i}_{j} \qquad \text{(decomposition)} $$

$$ {}^{d}_{e}\overset{\nabla}{t}{}^{i}_{j} = 2\,G\,{}^{d}_{e}d^{i}_{j} \qquad \text{(elastic relation)} $$

3.16

$$ \overline{\mathrm{II}} \leqslant \frac{2}{3}\,Y^{2} \qquad \text{(yield criterion)} $$

$$ {}^{d}_{p}d^{i}_{j} = \frac{\beta}{\sqrt{\overline{\mathrm{II}}}}\,{}^{d}_{e}t^{i}_{j} \qquad \text{(flow rule)} $$

In the next two sections the second and third equations of the above set will be expanded into physical components. The first and fourth equations pose no difficulty.

3.2.2. Two-Dimensional Equations in Physical Components

Expanding the second moment of the stress deviator in the two-dimensional case, the nonzero terms are

$$ \overline{\mathrm{II}} = 2\left\{\left({}^{d}_{e}t^{xx}\right)^{2} + \left({}^{d}_{e}t^{xz}\right)^{2} + \left({}^{d}_{e}t^{zz}\right)^{2} + {}^{d}_{e}t^{xx}\,{}^{d}_{e}t^{zz}\right\} \leqslant \frac{2}{3}\,Y^{2} \qquad 3.17 $$

where use has been made of the fact that the trace of a deviator vanishes.

The definition of objective stress rate is

$$ {}^{d}\overset{\blacktriangledown}{t}{}^{ij} = {}^{d}\overset{\bullet}{t}{}^{ij} - w^{i}{}_{r}\, {}^{d}t^{rj} - w^{j}{}_{r}\, {}^{d}t^{ir} \qquad 3.18 $$

where w_{ij} is the spin tensor defined as $w_{ij} = u_{[i,j]}$. Referring to the physical components of the velocity gradient given previously, the only nonzero component is

$$ w^{xz} = \frac{1}{2}\left(\frac{\partial u^{x}}{\partial z} - \frac{\partial u^{z}}{\partial x} \right) \qquad 3.19 $$

so that the physical components of the objective stress rate for both rectangular and cylindrical coordinates are

$$ \left.\begin{aligned} {}^{d}_{e}\overset{\blacktriangledown}{t}{}^{xx} &= \frac{\partial\, {}^{d}_{e}t^{xx}}{\partial t} - 2\, w^{xz}\, {}^{d}_{e}t^{xz} = 2\, G\, {}^{d}_{e}d^{xx} \\ {}^{d}_{e}\overset{\blacktriangledown}{t}{}^{xz} &= \frac{\partial\, {}^{d}_{e}t^{xz}}{\partial t} + w^{xz}\left({}^{d}_{e}t^{xx} - {}^{d}_{e}t^{zz} \right) = 2\, G\, {}^{d}_{e}d^{xz} \\ {}^{d}_{e}\overset{\blacktriangledown}{t}{}^{zz} &= \frac{\partial\, {}^{d}_{e}t^{zz}}{\partial t} + 2\, w^{xz}\, {}^{d}_{e}t^{xz} = 2\, G\, {}^{d}_{e}d^{zz} \end{aligned}\right\} \qquad 3.20 $$

It is unnecessary to refer to principal directions in order to determine the stress deviator. If principal components

and directions are needed, for example, to apply a fracture criterion, these can be found very simply. We note that the stress deviator matrix is

$$
{}^{d}_{e}t^{ab} = \begin{bmatrix} {}^{d}_{e}t^{xx} & 0 & {}^{d}_{e}t^{xz} \\ 0 & {}^{d}_{e}t^{yy} & 0 \\ {}^{d}_{e}t^{xz} & 0 & {}^{d}_{e}t^{zz} \end{bmatrix}
$$

so that one principal direction is the y direction with principal component ${}^{d}_{e}t^{yy}$ and the other two principal components are found by diagonalizing its cofactor

$$
{}^{d}_{e}t^{a} = \frac{1}{2}\left\{ \left({}^{d}_{e}t^{xx}\right) + \left({}^{d}_{e}t^{zz}\right) \pm \sqrt{\left({}^{d}_{e}t^{xx} - {}^{d}_{e}t^{zz}\right)^{2} + 4\left({}^{d}_{e}t^{xz}\right)^{2}} \right\} \qquad 3.21
$$

where $a = 1, 2$ respectively.

Components of the unit vectors corresponding to these principal values are then given by

$$
N^{x}_{a} = \frac{{}^{d}_{e}t^{xz}}{\sqrt{\left({}^{d}_{e}t^{xx} - {}^{d}_{e}t^{a}\right)^{2} - \left({}^{d}_{e}t^{xz}\right)^{2}}}
$$

3.22

$$
N^{z}_{a} = \frac{{}^{d}_{e}t^{xx} - {}^{d}_{e}t^{a}}{\sqrt{\left({}^{d}_{e}t^{xx} - {}^{d}_{e}t^{a}\right) - \left({}^{d}_{e}t^{xz}\right)^{2}}}
$$

These components are direction cosines of the principal directions. It is easily seen that the angles between the principal directions and the x axis are

$$\theta_a = \arctan \frac{{}^d_e t^{xx} - {}^d_e t^a}{{}^d_e t^{xz}} \qquad 3.23$$

where the two values of ${}^d_e t^a$ from equation 3.21 are used.

3.2.3 One-Dimensional Equations in Physical Components

In one dimension, the equations are somewhat simpler due to the absence of rotation. The yield condition reduces to

$$\bar{II} = ({}^d_e t^x)^2 + ({}^d_e t^y)^2 + ({}^d_e t^z)^2 \leq \frac{2}{3} Y^2 \qquad 3.24$$

while the elastic relation becomes.

$$\frac{\partial {}^d_e t^x}{\partial t} = 2 G \, {}^d_e d^x \qquad 3.25$$

For the rectangular ($\alpha = 1$) and spherical ($\alpha = 3$) cases, the symmetry of the motion leads to considerable simplification. Since

$${}^d_e t^y = {}^d_e t^z \qquad 3.26$$

and the condition

$$ {}_e^d t^x + {}_e^d t^y + {}_e^d t^z = 0 \qquad 3.27 $$

the yield condition immediately reduces to

$$ \overline{II} = \frac{3}{2} \left({}_e^d t^x \right)^2 \leqslant \frac{2}{3} Y^2 \qquad 3.28 $$

It is therefore unnecessary to refer to the rest of equations 3.16 when the material is at yield. When the material is elastic, equation 3.25 suffices to determine ${}_e^d t^x$.

For the cylindrical case ($\alpha = 2$) such simplification is not possible. It is thus necessary to solve the whole system of equations 3.16. The elastic relation in physical components becomes

$$ \frac{\partial {}_e^d t^x}{\partial t} = 2 G \, {}_e^d d^x $$

$$ \frac{\partial {}_e^d t^y}{\partial t} + 2 \frac{{}_e^d t^y u^x}{x} = 2 G \, {}_e^d d^y \qquad 3.29 $$

$$ \frac{\partial {}_e^d t^z}{\partial t} = 2 G \, {}_e^d d^z $$

It is unnecessary to use the second relation above. Using the property that the trace of a deviator vanishes to eliminate ${}_e^d t^y$ from the yield condition,

$$\bar{\Pi} = 2\left\{\left({}^{d}_{e}t^{x}\right)^{2} + {}^{d}_{e}t^{x}\,{}^{d}_{e}t^{z} + \left({}^{d}_{e}t^{z}\right)^{2}\right\} \leq \frac{2}{3}Y^{2} \qquad 3.30$$

3.2.4 Geometrical Representation of Stress

If the stress deviator is referred to principal axes, which in the one-dimensional case coincide with the coordinate axes, the shear components vanish. It is then possible to plot the stress state in a three dimensional rectangular coordinate system.[8] The condition that the trace of the stress deviator vanishes, equation 3.27, defines a plane, called the π plane, with a normal which has direction cosines $(1/\sqrt{3},\ 1/\sqrt{3},\ 1/\sqrt{3})$.

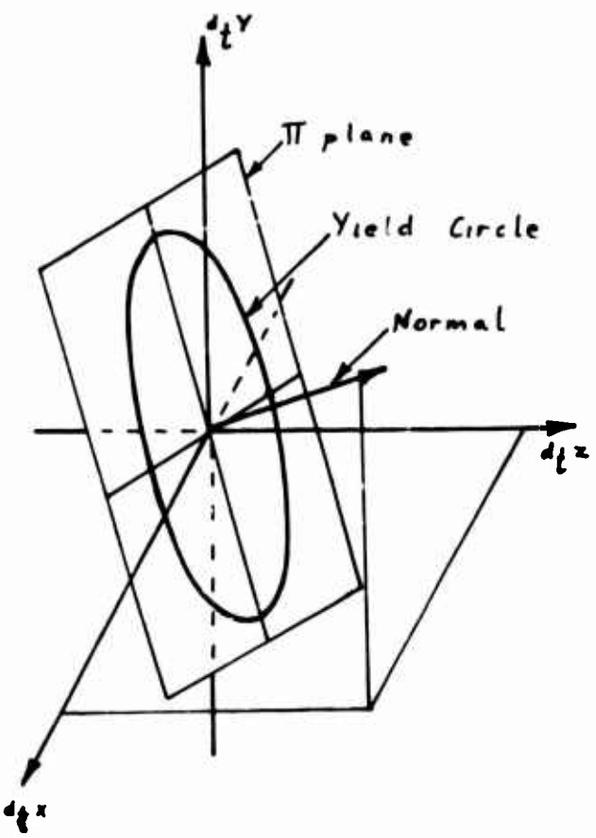

The yield condition, equation 3.24 defines a sphere of radius $\sqrt{\frac{2}{3}}Y$. Thus all attainable stress deviator states are limited to the π plane in a domain within a yield circle of radius $\sqrt{\frac{2}{3}}Y$. It is convenient to rotate the coordinate system so that the yield circle is in the plane of the paper, and to use polar coordinates to determine any given stress state P in this plane.

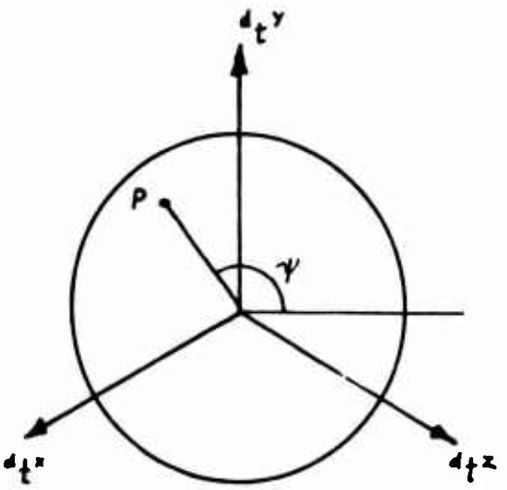

It is immediately evident from equation 3.24 that the radius vector is given by $\sqrt{\bar{II}}$. The angle between the radius vector, and the line formed by the intersection of the π plane and the $d_t^x - d_t^z$ coordinate plane is given by

$$\psi = \arctan\left(-\frac{\nu}{\sqrt{3}}\right) \qquad 3.31$$

where

$$\nu = \frac{2\,d_t^y - d_t^x - d_t^z}{d_t^x - d_t^z}$$

is Lode's variable. Using equation 3.27, this reduces simply to

$$\psi = \arctan \sqrt{3}\,\frac{d_t^x + d_t^z}{d_t^x - d_t^z} \qquad 3.32$$

It is clear that $\bar{II}$, ψ and p are sufficient to define any elastic stress state.

SECTION IV

STABILITY

4.1 Artificial Viscosity

Discontinuities or shocks may develop in solutions to the motion of perfect compressible fluids and solids. Such discontinuities lead to instabilities in the finite difference calculation. This problem is avoided by rendering the solution smooth and continuous everywhere by the introduction of artificial viscosity, so formulated that solutions are only affected in areas of very high gradients, i.e., in shock zones. Following von Neumann and Richtmyer[6] we choose a bulk viscosity coefficient dependent on the dilatation so that the viscous stress is negligible in areas of moderate gradient, i.e.,

$$(\lambda + 2/3\,\mu) = -\,b_1^2\,\rho\,d^k_k \qquad 4.1$$

in equation 3.3, where b_1 is a constant with dimensions of length. In some problems it is found desirable to include a linear viscous coefficient. Following Landshoff[9] this is formulated as

$$(\lambda + 2/3\,\mu) = b_2\,\rho\,c \qquad 4.2$$

where b_2 also has dimensions of length, and c is the sonic velocity of the medium. The viscous pressure can therefore be written, with the use of the continuity equation, as

$$q = b_1^2 \frac{\dot{\rho}^2}{\rho} + b_2 c \dot{\rho} \qquad 4.3$$

Since only compression shocks are possible, q is set equal to zero when $\dot{\rho} < 0$

Experience has shown that equivoluminal oscillations may occur in two-dimensional finite difference schemes, and a variety of artifices have been adopted to strengthen the viscous stress in the direction of maximum velocity gradient. This can be done elegantly by introducing a viscous stress deviator in a way analogous to the introduction of the viscous pressure above.

$$^{d}q^{i}_{j} = - b_3^2 \rho \left(^{d}d^{i}_{j}\right)^2 + b_4 \rho c \left(^{d}d^{i}_{j}\right) \qquad 4.4$$

Again, the viscous stress may be unnecessary on expansion, and may be set equal to zero when $^{d}d^{i}_{j} > 0$.

There is no difficulty in expanding equation 4.4 into three equations in physical components for the two-dimensional case. In the one-dimensional case it is sufficient to retain only the bulk viscosity.

4.2 Stability Criterion

The conditional stability of second order finite difference equations is well known.[6] In the finite difference scheme, quantities are sampled at discrete intervals in space (Δx , Δz) and time (Δt). The time increment cannot be chosen arbitrarily. If the time increment is too large, disturbances with wave lengths of the order of the mesh size tend to grow without bound. A variational analysis of the one dimensional finite difference equations (Appendix A) in which solutions are sought in the form

$$\delta u = \delta u_0 \, e^{ikx + at} \tag{4.5}$$

etc. suggests that a sufficient condition for stability is

$$\Delta t \leq \frac{\Delta x}{(1+2b_2)c + 4b_1^2 |\Delta u|} \tag{4.6}$$

Deviator viscous stresses have been omitted in this development, since they are in general smaller than the spherical viscous terms. No difficulty has been encountered on this account, presumably because equation 4.6 is somewhat more stringent than the necessary condition.

A complete stability analysis has not been carried out for the two-dimensional finite difference equations (Appendix B). However, an analogous form of stability criterion has been found useful. Note that in one dimension the continuity equation can be written (equation 2.2)

$$\frac{\Delta u}{\Delta x} = - \frac{\dot{\rho}}{\rho} \qquad 4.7$$

Taking $\sqrt{A}$ as a measure of mesh size, where A is the area of a mesh, equation 4.6 becomes

$$\Delta t \leq \frac{\sqrt{A}}{(1 + 2 b_1) c + 4 b_1^2 \sqrt{A} \left| \frac{\dot{\rho}}{\rho} \right|} \qquad 4.8$$

Despite the fact that $\sqrt{A}$ is not a good approximation to the mesh size for a highly distorted mesh, the use of this equation has not, so far, led to any stability problems. This presumably arises from the fact that the error in the numerator partially offsets the error in the denominator.

SECTION V

FINITE-DIFFERENCE ANALOGS

The differential equations given in the previous section are to be integrated numerically. The derivative terms are replaced by finite difference analogs to produce a set of algebraic equations which are solved in a stepwise manner to produce the desired solution. The principal difficulty concerns the choice of finite difference analogs to the partial derivatives.

In one space dimension centered difference expressions correct to second order will be used. In two space dimensions, a variety of difference analogs, presumably of the same order of approximation, have appeared in the literature. Some of these have been compared in another report.[10] Here short derivations of the analogs which were found to be most suitable are given. Application of these to develop the complete finite difference equations in one and two space dimensions is postponed to the appendices.

In one dimension, the usual approach is to use Taylor's expansion. Consider an arbitrary quantity ψ varying with an independent variable x (which may represent time, or distance in one space dimension). We wish to find the gradient of ψ at a point 0 given values of ψ at neighboring points 1 and 2 finite distances from 0. Applying

Taylor's expansion,

$$\psi_1 = \psi_0 + (x_1 - x_0)\frac{\partial \psi}{\partial x} + \frac{1}{2}(x_1 - x_0)^2 \frac{\partial^2 \psi}{\partial x^2} + \frac{1}{6}(x_1 - x_0)^3 \frac{\partial^3 \psi}{\partial x^3} + \cdots \qquad 5.1$$

$$\psi_2 = \psi_0 + (x_2 - x_0)\frac{\partial \psi}{\partial x} + \frac{1}{2}(x_1 - x_0)^2 \frac{\partial^2 \psi}{\partial x^2} + \frac{1}{6}(x_1 - x_0)^3 \frac{\partial^3 \psi}{\partial x^3} + \cdots$$

Solving these for $\frac{\partial \psi}{\partial x}$,

$$\frac{\partial \psi}{\partial x} = \frac{\psi_2 - \psi_1}{x_2 - x_1} - \frac{\partial^2 \psi}{\partial x^2}\delta_{x21} - \frac{\partial^3 \psi}{\partial x^3}\left[\frac{(x_2 - x_1)^2}{24} + \frac{1}{2}\delta_{x21}\right] - \cdots \qquad 5.2$$

where $\delta_{x21} = \frac{1}{2}(x_2 + x_1) - x_0$ is a measure of the assymmetry of the mesh. If the mesh is nearly symmetric the second order term is negligible, and if the mesh size is small, the higher order terms are negligible, and

$$\frac{\partial \psi}{\partial x} = \frac{\psi_2 - \psi_1}{x_2 - x_1} \qquad 5.3$$

It is clear that the truncation error grows as the mesh becomes more asymmetric.

Precisely the same reasoning has been used to construct a finite difference analog to partial derivatives in two space dimensions. Consider an arbitrary quantity ψ varying with two independent variables x and z. We wish to find the gradients of ψ in the x and z directions at point 0 given

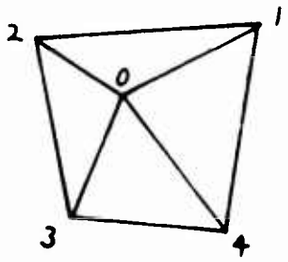

values of Ψ at four neighboring points 1 2 3 4 finite distances from 0. Applying Taylor's theorem we obtain four equations of the type

$$\Psi_1 = \Psi_0 + (x_1 - x_0)\frac{\partial \Psi}{\partial x} + (z_1 - z_0)\frac{\partial \Psi}{\partial z}$$

5.4

$$+ \tfrac{1}{2}(x_1 - x_0)^2 \frac{\partial^2 \Psi}{\partial x^2} + \tfrac{1}{2}(x_1 - x_0)(z_1 - z_0)\frac{\partial^2 \Psi}{\partial x \partial z} + \tfrac{1}{2}(z_1 - z_0)^2 \frac{\partial^2 \Psi}{\partial z^2} + \cdots$$

Kolsky[11] suggested solving this overdetermined system of equations by first solving for ($\Psi_1 - \Psi_2$) and ($\Psi_2 - \Psi_4$) giving two equations

$$(\Psi_1 - \Psi_3) = \frac{\partial \Psi}{\partial x}(x_1 - x_3) + \frac{\partial \Psi}{\partial z}(z_1 - z_3) + R_{13}$$

5.5

$$(\Psi_2 - \Psi_4) = \frac{\partial \Psi}{\partial x}(x_2 - x_4) + \frac{\partial \Psi}{\partial z}(z_2 - z_4) + R_{24}$$

where the remainder terms again depend on the assymmetry of the mesh and the mesh size. Again, providing that the assymmetry and mesh size are both small, the remainder terms may be neglected in comparision with the first order terms. Solving for the gradients in this case

$$\frac{\partial \Psi}{\partial x} = \frac{1}{2A}\left\{(\Psi_2 - \Psi_4)(z_1 - z_3) - (\Psi_1 - \Psi_3)(z_2 - z_4)\right\}$$

5.6

$$\frac{\partial \Psi}{\partial z} = \frac{-1}{2A}\left\{(\Psi_2 - \Psi_4)(x_1 - x_3) - (\Psi_1 - \Psi_3)(x_2 - x_4)\right\}$$

where

$$A = \frac{1}{2}\left\{(z_1 - z_3)(x_2 - x_4) - (z_2 - z_4)(x_1 - x_3)\right\}$$

It is seen that A represents the area of the quadrilateral 1 2 3 4.

It is interesting to note that an identical result may be obtained in another way. Green's Transformation in two dimensions may be written

$$\int_A \psi_{,i}\, da = \oint_S \psi\, n_i\, ds \qquad 5.7$$

where n_i is the unit exterior normal to the surface S enclosing an area A. In component form this becomes

$$\oint_S \psi\, dz = \int_A \frac{\partial \psi}{\partial x}\, da = \left(\frac{\partial \psi}{\partial x}\right)_{AVE} A$$

$$-\oint_S \psi\, dx = \int_A \frac{\partial \psi}{\partial z}\, da = \left(\frac{\partial \psi}{\partial z}\right)_{AVE} A \qquad 5.8$$

where the gradients have been averaged over the area A. Applying these relations to the quadrilateral 1 2 3 4 surrounding point 0, we find that the average gradients may be expressed as

$$\frac{\partial \psi}{\partial x} = \frac{1}{A}\left\{\psi_{\overline{12}}(z_1 - z_2) + \psi_{\overline{23}}(z_2 - z_3) + \psi_{\overline{34}}(z_3 - z_4) + \psi_{\overline{41}}(z_4 - z_1)\right\}$$

$$\frac{\partial \psi}{\partial z} = \frac{-1}{A}\left\{\psi_{\overline{12}}(x_1 - x_2) + \psi_{\overline{23}}(x_2 - x_3) + \psi_{\overline{34}}(x_3 - x_4) + \psi_{\overline{41}}(x_4 - x_1)\right\} \qquad 5.9$$

where $\psi_{\overline{12}}$ is the average of ψ over the side 1 2 etc. if we write

$$\psi_{\overline{12}} = \frac{1}{2}\left(\psi_1 + \psi_2\right) \quad etc.$$

the above equations 5.9 immediately reduce to the previous equation 5.6.

Both forms (equations 5.6 and 5.9) will be found useful in developing the finite difference equations in two space dimensions. It is clear from their development, however, that the truncation error due to neglect of the higher order terms must depend on the asymmetry of the mesh. The truncation error has been investigated in another report, and has been found to become comparable to the terms which are retained even for moderate distortions of the mesh.

SECTION VI

RESULTS

A few illustrative calculations are presented in this section. While the results are suggestive of the role of material strength in plastic wave propagation, considerable work remains to be done, particularly on the representation of material properties, before quantitative information can be extracted.

Results using the one-dimensional finite difference method for the face-on impact of two aluminum plates are shown in Figs.1 through 4. The configurations were chosen to correspond to experimental data reported by Curren.[2] The material constants used were

ρ_0 = 2.78 gm/cm^3	Y = 2.76 kb	
k_0 = 764 kb	h_0 = 5.473	g_0 = 286 kb
k_1 = 1.014	h_1 = 1.0	g_1 = 5.86
k_2 = -.236	h_2 = 1.0	g_2 = 8.44
k_3 = -.513	h_3 = 1.0	g_3 = 0.0

Figure 1 shows print plots of stress profiles for a driver plate velocity of 1.9 km/sec, while Fig. 2 shows corresponding results when the yield stress is set to zero. Figures 3 and 4 show initial rear surface velocities of the target plate upon reflection of the stress wave as a function of target plate thickness (in terms of driver plate thickness), for driver plate velocities of 1.9 km/sec and 1.2 km/sec respectively. Also shown are experimental data of Curran,[2] and results of the

hydrodynamic theory of Fowles.[15]

The computer solutions for zero strength ($Y = 0$) fall well below Fowles' prediction. This may be ascribed to differences in the fit to the hugoniot, and the fact that Fowles did not account for entropy changes, in so far as he used the hugoniot for the expansion instead of an isentrope. The computer solutions including material strength fall well below the zero strength solutions, but not sufficiently to agree with the experimental data. The remaining disagreement may well be due to an increase in yield strength with compression as suggested by Curran.

When material strength is included, it is seen from Fig. 1 that an elastic release wave with an amplitude of about 15 kb moves into the compressed material behind the shock with the local elastic wave velocity. The existence of a 15 kb elastic release wave, despite the fact that the yield stress is taken constant at 2.76 kb, can be explained by referring to Fig. 5 which shows a schematic of the elastic plastic constitutive relation neglecting hysteresis due to the entropy change in the shock. On loading, a stress-strain path lying a distance $\frac{2}{3}Y$ above the hydrostatic curve is followed (0 A B C in Fig. 5). On release of stress from state C, path C D E is followed, so that an elastic release wave of amplitude C D is generated. The amplitude of the elastic release wave is determined

by the slope of segment C D, relative to the slope of the hydrostats. The slope of C D is ($K + 4/3\ G$) while the slope of the hydrostat is (K). Thus the relative slope depends on the shear modulus G. At the same time the velocity of the elastic release wave is given by

$$c_e = \sqrt{(K + 4/3\, G)/\rho}$$

Thus, if the value of G is increased, the elastic wave amplitude is decreased but its velocity is increased. Higher attenuation results from a larger elastic release wave amplitude, but also from a release wave of higher velocity. Thus the two effects offset each other to some extent, and some variation in G does not materially affect the results, as found by Jones.[17]

Once the elastic release wave has reached the loading shock, the shock amplitude is reduced. As the reduced amplitude shock propagates, the material is now loaded to a lower stress (state B, Fig. 5). When the release wave reaches this material, a new elastic release wave will appear (corresponding to segment B E, Fig. 5) and the attenuation process will be repeated.

Results, using the one-dimensional finite difference method, for the response of an aluminum sphere 18 cm in diameter containing a concentric spherical cavity 3.4 cm in diameter filled with Pentolite are shown in Fig. 6 (not all mesh points are plotted). The configuration was chosen to correspond to experimental data obtained at the Ballistics Research Laboratory.[18] The

material constants for the aluminum were identical to those used above, while the material constants for the Pentolite were taken to be

$\rho_0 = 1.714$ gm/cm^3 $\qquad$ $\rho_1 = 2.333$ gm/cm^3

$\gamma = 1.77$ $\qquad$ $p_1 = 290.289$ kb.

$\beta = 2.77$

$D = 7.991$ km/sec

It can be seen that the results for zero strength ($Y = 0$) and a strength $Y = 2.76$ kb do not differ very materially except at late times. The difference is sufficient however to cause a drastic difference in spall behaviour. The elastic-plastic case ($Y = 2.76$ kb) showed 3 spalls at radii of 7.55, 5.70 and 3.90 cm. respectively, while the hydrodynamic case ($Y = 0$) showed several spalls, the outermost occuring at a radius of 8.55 cm. Great care is necessary in interpreting spall results from finite difference calculations, since these depend to some extent on the choice of mesh size and artificial viscosity co-efficients. The above results should be regarded as preliminary.

In Fig. 7 is plotted the cavity radius vs. time for $Y = 0$ and $Y = 2.78$ kb. The cavity radius grows somewhat more slowly when material strength is included. The cavity radius at 20 microseconds was computed to be 2.68 cm, which might be compared with the final cavity radius of about 2.95 cm found in the experiment. It is clear that the cavity grows for times in

excess of 100 microseconds, which is long compared to the time required for the initial shock to reach the outside boundary of the aluminum (about 15 microseconds).

Preliminary results using the two-dimensional finite difference method for the end-on impact of a finite length aluminum cylinder on a smooth wall (or symmetry plane) are shown in Figs. 8 and 9. The material constants for the aluminum were identical to those used above.

In Fig. 8 are shown deformed material coordinates at various stages during the motion, while in Fig. 9 are shown corresponding isometric (Lagrangian) plots of the hydrostatic pressure. The effects of lateral release waves are clearly observable.

Appendix A

One Dimensional Finite Difference Equations

A.1 Equations of Motion

Consider only discrete points in space finite distances Δx apart and denote the initial coordinate of the jth such point x_j^o. Similarly, consider only discrete times finite increments Δt apart, and denote the nth such time t^n. We are then concerned with positions and accelerations of these points at these times, denoting by x_j^n and a_j^n the position and acceleration of the jth point at the nth time. Other quantities, such as pressure, density, stresses,etc.,are averaged over the intervals Δx and denoted by $p_{j+1/2}^n$, $\rho_{j+1/2}^n$, etc. We suppose that quantities vary so slowly that linear interpolation is justified,e.g.,

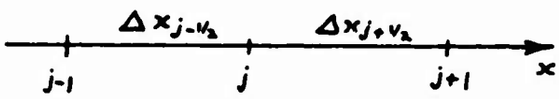

$$\psi_{j+1/2}^n = \frac{1}{2}\left(\psi_{j+1}^n + \psi_j^n\right) \qquad \text{A.1}$$

and similarly in time

$$\psi_j^{n+1/2} = \frac{1}{2}\left(\psi_j^{n+1} + \psi_j^n\right) \qquad \text{A.2}$$

Such linear interpolation is in accord with the approximations involved in the finite difference analogs to partial derivatives correct to second order,i.e.,

$$\frac{\partial \psi}{\partial x} = \frac{\psi_{j+1/2}^n - \psi_{j-1/2}^n}{x_{j+1/2}^n - x_{j-1/2}^n} \qquad \text{A.3}$$

$$\frac{\partial \psi}{\partial t} = \frac{\psi_j^{n+1/2} - \psi_j^{n-1/2}}{t^{n+1/2} - t^{n-1/2}} \qquad \text{A.4}$$

Simplifying the notation, the momentum equation will be written

$$a = -\frac{1}{\rho}\frac{\partial(\sigma + q)}{\partial t} + (\alpha - 1)\frac{\phi}{\rho x}$$

where we have written $a = a^x$, $\sigma = -{}_e t^x$, $\phi = {}_e t^x - {}_e t^y$ and where body forces have been temporarily omitted. Applying the above principles, the finite difference form is

$$a_j^n = -2\left\{\frac{(\sigma_{j+1/2}^n - \sigma_{j-1/2}^n) + (q_{j+1/2}^n - q_{j-1/2}^n)}{\rho_{j+1/2}^n(x_{j+1}^n - x_j^n) + \rho_{j-1/2}^n(x_j^n - x_{j-1}^n)}\right. \qquad \text{A.6}$$

$$\left. - (\alpha - 1)\frac{\phi_{j+1/2}^n + \phi_{j-1/2}^n}{\rho_{j+1/2}^n(x_{j+1}^n + x_j^n) + \rho_{j-1/2}^n(x_j^n + x_{j-1}^n)}\right\}$$

The velocity and coordinate are given by

$$u_j^{n+1/2} = u_j^{n-1/2} + \tfrac{1}{2}(\Delta t^{n+1/2} + \Delta t^{n-1/2})\, a_j^n \qquad \text{A.7}$$

$$x_j^{n+1} = x_j^n + \Delta t^{n+1/2}\, u_j^{n+1/2} \qquad \text{A.8}$$

It is simplest to take the continuity equation in integral form, whence

$$\rho_{j+1/2}^{n+1} = \frac{m_{j+1/2}}{\left(x_{j+1}^{n+1}\right)^{\alpha} - \left(x_{j}^{n+1}\right)^{\alpha}} \qquad \text{A.9}$$

where

$$m_{j+1/2} = \left\{ \left(x_{j+1}'\right)^{\alpha} - \left(x_{j}'\right)^{\alpha} \right\} \rho_{j+1/2}'$$

is a constant for each mesh point.

A.2 Artificial Viscosity

In order to link the width of shock zones to the mesh size, the artificial viscosity coefficients are set proportional to the mesh size, so that the artificial viscosity becomes

$$q_{j+1/2}^{n+1} = \rho_{j+1/2}^{n+1} \left\{ B_2 \left(x_{j+1}^{n+1} - x_{j}^{n+1}\right) c_{j+1/2}^{n} \left(\frac{\dot{\rho}}{\rho}\right) + \left[B_1 \left(x_{j+1}^{n+1} - x_{j}^{n+1}\right)\left(\frac{\dot{\rho}}{\rho}\right)\right]^2 \right\}$$

$$\text{for} \quad \left(\frac{\dot{\rho}}{\rho}\right) > 0$$

$$q_{j+1/2}^{n+1} = 0 \qquad \text{for} \quad \left(\frac{\dot{\rho}}{\rho}\right) \leq 0$$

where

$$\frac{\dot{\rho}}{\rho} = \frac{2\left(\rho_{j+1/2}^{n+1} - \rho_{j+1/2}^{n}\right)}{\Delta t^{n+1/2}\left(\rho_{j+1/2}^{n+1} + \rho_{j+1/2}^{n}\right)}$$

The sound speed does not change very rapidly so that the use of $c_{j+1/2}^{n}$ in this equation does not introduce any difficulties.

A.3 Fluid Constitutive Equation

Several equation of state options are available. It is convenient to deal with a fluid separately. If the flow is isentropic, an equation in the form

$$ {}_eP = f(\rho) \qquad \text{A.11} $$

fitted to the isentrope suffices. For more general motions, the relation

$$ {}_eP = f_1(\rho) + \mathcal{E} f_2(\rho) \qquad \text{A.12} $$

where f_1 and f_2 will be expressed in terms of $\eta = (\rho - \rho_0)/\rho$

$$ f_1 = k_0 \eta \left\{ 1 + k_1 \eta + k_2 \eta^2 + \cdots \right\} $$

$$ f_2 = h_0 \left\{ 1 + h_1 \eta + h_2 \eta^2 + \cdots \right\} $$

is combined with the energy equation, which in finite difference form is

$$ \mathcal{E}^{n+1}_{j+1/2} = \mathcal{E}^{n}_{j+1/2} + \tfrac{1}{2}\left({}_eP^{n+1}_{j+1/2} + {}_eP^{n}_{j+1/2} + q^{n+1}_{j+1/2} + q^{n}_{j+1/2} \right) \frac{\Delta\rho}{\rho^2} \qquad \text{A.13} $$

where

$$ \frac{\Delta\rho}{\rho^2} = 4 \frac{\left(\rho^{n+1}_{j+1/2} - \rho^{n}_{j+1/2} \right)}{\left(\rho^{n+1}_{j+1/2} + \rho^{n}_{j+1/2} \right)^2} $$

Heat conduction and energy source terms have been temporarily omitted. Substituting A.12 at t^{n+1} into A.13 provides an explicit equation for the internal energy

$$ \mathcal{E}^{n+1}_{j+1/2} = \frac{\mathcal{E}^{n}_{j+1/2} + \tfrac{1}{2}\left(f_{1\,j+1/2}^{n+1} + {}_eP^{n}_{j+1/2} + q^{n+1}_{j+1/2} + q^{n}_{j+1/2} \right) \frac{\Delta\rho}{\rho^2}}{1 - \tfrac{1}{2} f_{2\,j+1/2}^{n+1} \frac{\Delta\rho}{\rho^2}} \qquad \text{A.14} $$

The pressure can then be found from equation A.12 and $\sigma = {}_e p$ $\phi = 0$. The sound speed is given by

$$\left(c^{n+1}_{j+1/2}\right)^2 = \frac{1}{\rho^{n+1}_{j+1/2}}\left\{\left(\rho\frac{\partial f_1}{\partial \rho}\right)^{n+1}_{j+1/2} + \mathcal{E}^{n+1}_{j+1/2}\left(\rho\frac{\partial f_2}{\partial \rho}\right)^{n+1}_{j+1/2} + f^{n+1}_{2\,j+1/2}\, {}_e p^{n+1}_{j+1/2}/\rho^{n+1}_{j+1/2}\right\} \qquad \text{A.15}$$

where

$$\rho\frac{\partial f_1}{\partial \rho} = k_0(1-\eta)\left\{1 + 2k_1\eta + 3k_2\eta^2 + \cdots\right\}$$

$$\rho\frac{\partial f_2}{\partial \rho} = h_0(1-\eta)\left\{h_1 + 2h_2\eta + 3h_3\eta^2 + \cdots\right\}$$

A.4 Elastic Perfectly Plastic Constitutive Equation

The stretching deviator is

$$\left({}^d d^x\right)^{n+1/2}_{j+1/2} = \frac{2\left(u^{n+1/2}_{j+1} - u^{n+1/2}_{j}\right)}{\left(x^{n+1}_{j+1} + x^{n}_{j+1}\right) - \left(x^{n+1}_{j} + x^{n}_{j}\right)} + \frac{1}{3}\frac{\dot{\rho}}{\rho} \qquad \text{A.16}$$

and the elastic stress deviator becomes

$${}^d_e t^x = \left({}^d_e t^x\right)^n_{j+1/2} + 2\Delta t^{n+1/2} G^{n+1/2}_{j+1/2}\left({}^d d^x\right)^{n+1/2}_{j+1/2} \qquad \text{A.17}$$

where we will take the shear modulus to depend on compression

$$G = g_0\left\{1 + g_1\eta + g_2\eta^2 + \cdots\right\}$$

For $\alpha = 1$ or 3, the yield condition reduces to

$$\bar{\Pi} = \frac{3}{2}\left({}^{d}_{e}t^{x}\right)^{2} \qquad \text{A.18}$$

Then

If $\quad \bar{\Pi} \leq \frac{2}{3} Y^{2} \qquad \left({}^{d}_{e}t^{x}\right)^{n+1}_{j+1/2} = {}^{d}_{e}t^{x}$

If $\quad \bar{\Pi} > \frac{2}{3} Y^{2} \qquad \left({}^{d}_{e}t^{x}\right)^{n+1}_{j+1/2} = \mathrm{Sgn}\, {}^{d}_{e}t^{x} \cdot \frac{2}{3} Y$

Then
$$\phi = {}^{d}_{e}t^{x} - {}^{d}_{e}t^{y} = \frac{3}{2}\left({}^{d}_{e}t^{x}\right) \qquad \text{A.19}$$

and the deviator stress work is simply

$$\Delta\, {}^{d}\mathcal{E} = \frac{3}{2}\, \Delta t^{n+1/2} \left({}^{d}d^{x}\right)^{n+1/2}_{j+1/2} \frac{\left({}^{d}_{e}t^{x}\right)^{n+1}_{j+1/2} + \left({}^{d}_{e}t^{x}\right)^{n}_{j+1/2}}{\rho^{\,n+1}_{j+1/2} + \rho^{\,n}_{j+1/2}} \qquad \text{A.20}$$

This is used in computing the pressure below. For $\alpha = 2$ a more elaborate procedure is required. We compute the z component of stretching and stress deviators

$$\left({}^{d}d^{z}\right)^{n+1/2}_{j+1/2} = \frac{1}{3}\,\frac{\dot{\rho}}{\rho} \qquad \text{A.21}$$

$${}^{d}_{e}t^{z} = \left({}^{d}_{e}t^{z}\right)^{n}_{j+1/2} + 2\,\Delta t^{n+1/2}\, G^{n+1/2}_{j+1/2} \left({}^{d}d^{z}\right)^{n+1/2}_{j+1/2} \qquad \text{A.22}$$

These equations are, of course only valid if the material is elastic. When the material is plastic it is necessary to solve the set of simultaneous equations for the unknown stress components and proportionality factor ζ . Due to the quadratic form of the yield condition, this cannot be done explicitly. Instead, a forward differencing scheme used by Wilkins and Giroux,[3] and Maenchen and Sack[4] is used. Referring to the Π plane representation,

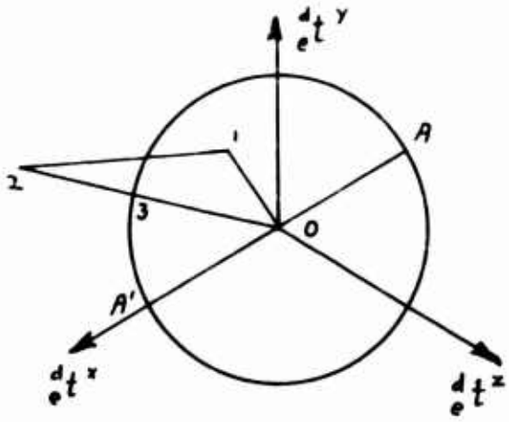

we consider an elastic stress state 1 at t^n, and use equations A.16, A.17, A.21 and A.22 to compute a new elastic stress state 2 at t^{n+1}. The second moment is then computed using

$$\bar{\Pi} = 2\left\{\left({}_e^dt^x\right)^2 + {}_e^dt^x \cdot {}_e^dt^z + \left({}_e^dt^z\right)^2\right\}$$

Then if

$$\bar{\Pi} \leq \frac{2}{3} Y^2$$

Use $\left({}_e^dt^x\right)^{n+1}_{j+1/2} = {}_e^dt^x \qquad \left({}_e^dt^z\right)^{n+1}_{j+1/2} = {}_e^dt^z$ A.23

since the material is still elastic. However,

if $\bar{\Pi} > \frac{2}{3} Y^2$

the material has become plastic as shown in the diagram. Approximately the correct yield stress is achieved by using

$$\left({}_e^dt^x\right)^{n+1}_{j+1/2} = \sqrt{\frac{\frac{2}{3}Y^2}{\bar{\Pi}}}\ {}_e^dt^x \qquad \left({}_e^dt^z\right)^{n+1}_{j+1/2} = \sqrt{\frac{\frac{2}{3}Y^2}{\bar{\Pi}}}\ {}_e^dt^z \qquad \text{A.24}$$

which in effect computes the stress state at point 3 on the yield surface on a radius vector from state 2. The procedure is only valid when the change in Lode's angle is small. It might be noted that when $\alpha = 1$ or 3, the symmetry condition ${}_e^dt^y = {}_e^dt^z$ limits the attainable stress states to the straight line AA' in the diagram above, and the procedure given for finding the stress deviators for this case does not involve this approximation. Then $\phi = 2\,{}_e^dt^x + {}_e^dt^z$ and

$$\Delta^d \mathcal{E} = \frac{\Delta t^{n+1/2}}{\rho^{n+1}_{j+1/2} + \rho^{n}_{j+1/2}} \left[\left\{ \left({}^d_e t^x \right)^{n+1}_{j+1/2} + \left({}^d_e t^x \right)^{n}_{j+1/2} \right\} \left\{ 2 \left({}^d d^x \right)^{n+1/2}_{j+1/2} + \left({}^d d^z \right)^{n+1/2}_{j+1/2} \right\} \right. \qquad \text{A.25}$$

$$\left. + \left\{ \left({}^d_e t^z \right)^{n+1}_{j+1/2} + \left({}^d_e t^z \right)^{n}_{j+1/2} \right\} \left\{ 2 \left({}^d d^z \right)^{n+1/2}_{j+1/2} + \left({}^d d^x \right)^{n+1/2}_{j+1/2} \right\} \right]$$

Finally the hydrostatic pressure is found as for a fluid, but including the deviator stress work in the energy equation A.14

$$\mathcal{E}^{n+1}_{j+1/2} = \frac{\mathcal{E}^{n}_{j+1/2} + \frac{1}{2} \left(f_1{}^{n+1}_{j+1/2} + {}_e p^{n}_{j+1/2} + q^{n+1}_{j+1/2} + q^{n}_{j+1/2} \right) \frac{\Delta \rho}{\rho^2} + \Delta^d \mathcal{E}}{1 - \frac{1}{2} f_2{}^{n+1}_{j+1/2} \frac{\Delta \rho}{\rho^2}} \qquad \text{A.26}$$

The pressure is found from equation A.12 and $\sigma = {}_e p - {}^d_e t^x$
The elastic sound speed may be taken as $\sqrt{1.5}$ times the value given in equation A.15

A.5 High Explosive Constitutive Equation

In order to force the detonation front to move at the proper velocity the following scheme is adopted. The time at which burning is initiated in a particular mesh will be

$$t^b_{j+1/2} = \frac{x^o_j - x^o_D}{D} \qquad \text{A.27}$$

where x^o_D is the initial position of the detonation point (the detonation is considered to be initiated to the left, or smallest

x_j^o), and D is the detonation wave velocity. In order to spread the detonation front over several meshes, a burn fraction is defined as

$$F_{j+1/2}^{n+1} = 0 \qquad \text{for} \quad t^{n+1} \leq t_{j+1/2}^{b}$$

A.28

$$F_{j+1/2}^{n+1} = \frac{D}{B_s \, \Delta x^o} \left(t^{n+1} - t_{j+1/2}^{b} \right) \qquad \text{for} \quad t^{n+1} > t_{j+1/2}^{b}$$

where $0 \leq F \leq 1$, and B_s is a constant which determines the thickness of the shock front. If we now take

$$eP_{j+1/2}^{n+1} = F_{j+1/2}^{n+1} \left(f_{1\,j+1/2}^{n+1} + \mathcal{E}_{j+1/2}^{n+1} \; f_{2\,j+1/2}^{n+1} \right) \qquad \text{A.29}$$

the pressure is maintained zero until the precomputed detonation time, and rises smoothly until $F = 1$. Since $F = 1$ for all times thereafter, equation A.29 provides the correct equation of state of the explosion products for the subsequent motion.

Solving equation A.29 together with the energy equation A.13 for a fluid provides the equation for the internal energy

$$\mathcal{E}_{j+1/2}^{n+1} = \frac{\mathcal{E}_{j+1/2}^{n} + \frac{1}{2}\left(F_{j+1/2}^{n+1} \; f_{j+1/2}^{n+1} + eP_{j+1/2}^{n} + q_{j+1/2}^{n+1} + q_{j+1/2}^{n} \right) \frac{\Delta\rho}{\rho^2}}{1 - \frac{1}{2} F_{j+1/2}^{n+1} \; f_{2\,j+1/2}^{n+1} \; \frac{\Delta\rho}{\rho^2}} \qquad \text{A.30}$$

The pressure is then found from equation A.29.

Choosing a polytropic law to describe isentropes and using the Mie-Grueneisen assumption to generalise to other nearby states, f_1 and f_2 can be expressed as

$$f_1 = \kappa \rho^{\beta}$$

$$f_2 = \gamma \rho \qquad \text{A.31}$$

where κ , β and γ are material constants. For the simple polytropic gas, the expression for the sound speed, equation A.15, reduces simply to

$$\left(c^{n+1}_{j+1/2}\right)^2 = \gamma \frac{{}_{e}P^{n+1}_{j+1/2}}{\rho^{n+1}_{j+1/2}} \qquad \text{A.32}$$

Other more elaborate forms for f_1 and f_2 may, of course, be used if deemed necessary.

A.6 Energy Checks

It is often desirable to study momentum and energy of individual meshes, or summed over portions or the whole of the material in the problem. The finite difference expressions below are collected for convenience, and are incorporated in a special subroutine only when required for diagnostic purposes.

The mass in a mesh is given by

$$M_{j+1/2} = k' \, m_{j+1/2} \qquad \text{A.33}$$

where

$k' = 1$	for	$\alpha = 1$
$k' = \pi$	for	$\alpha = 2$
$k' = \frac{4}{3}\pi$	for	$\alpha = 3$

Thus the momentum in a mesh is

$$H^{n+1/2}_{j+1/2} = M_{j+1/2}\left(\frac{u^{n+1/2}_{j+1} + u^{n+1/2}_{j}}{2}\right) \qquad \text{A.34}$$

The kinetic energy is

$$K_{j+1/2}^{n+1/2} = \frac{1}{2} M_{j+1/2} \left(\frac{u_{j+1}^{n+1/2} + u_j^{n+1/2}}{2} \right)^2 \qquad \text{A.35}$$

while the internal energy is

$$E_{j+1/2}^{n+1/2} = \frac{1}{2} M_{j+1/2} \left(\mathcal{E}_{j+1/2}^{n+1} + \mathcal{E}_{j+1/2}^{n} \right) \qquad \text{A.36}$$

It is useful to sum kinetic and internal energy over the material. Then if energy is conserved

$$\sum_j \left(K_{j+1/2}^{n+1/2} + E_{j+1/2}^{n+1/2} \right) - \sum_j \left(K_{j+1/2}^{n-1/2} + E_{j+1/2}^{n-1/2} \right) = \mathcal{W}^{n+1/2} + \mathcal{Q}^{n+1/2} \qquad \text{A.37}$$

where $\mathcal{W}^{n+1/2}$ is the surface work done from time t^n to time t^{n+1} (for example by a surface pressure) and $\mathcal{Q}^{n+1/2}$ is the nonmechanical energy addition in this time interval (for example, chemical energy in an explosive). This provides a very useful check on the calculation.

It is sometimes useful, in studying a particular motion in detail, to consider the energy distribution in various modes. Considering the time interval t^n to t^{n+1} in each case, the spherical elastic stress work done in a mesh is

$$\Delta \overset{\circ}{{}_e E}_{j+1/2}^{n+1/2} = \frac{1}{2} M_{j+1/2} \left({}_e P_{j+1/2}^{n+1} + {}_e P_{j+1/2}^{n} \right) \frac{\Delta \rho}{\rho^2} \qquad \text{A.38}$$

while the spherical viscous stress work is

$$\Delta \overset{\circ}{{}_q E}_{j+1/2}^{n+1/2} = \frac{1}{2} M_{j+1/2} \left(q_{j+1/2}^{n+1} + q_{j+1/2}^{n} \right) \frac{\Delta \rho}{\rho^2} \qquad \text{A.39}$$

The plastic stress work can be estimated in a manner consistent with the forward differencing scheme used in the constitutive equation.[4] Referring to the diagram in Section A.4, note that the plastic stretching deviator is related to the increment in stress between states 2 and 3, i.e.,

$$ {}_p^d d^a = \frac{1}{2G} \frac{{}_2^d t^a - {}_3^d t^a}{\Delta t} \qquad \text{A.40} $$

The plastic stress work per unit mass is thus approximately

$$ {}_p^d \dot{\varepsilon} = \frac{1}{\rho} {}_3^d t^a \, {}_p^d d^a = \frac{1}{2G\rho\Delta t} \left({}_2^d t^a - {}_3^d t^a \right) {}_3^d t^a \qquad \text{A.41} $$

where summation is implied over the index a. Using equation A.24 this becomes

$$ {}_p^d \dot{\varepsilon} = \frac{1}{2G\rho\Delta t} \left\{ \sqrt{\frac{\bar{\mathrm{II}}}{\frac{2}{3}Y^2}} - 1 \right\} {}_3^d t^a \, {}_3^d t^a \qquad \text{A.42} $$

Since state 3 is at yield, the second moment of the stress tensor at 3 is $\frac{2}{3}Y^2$. In finite difference form the plastic work done is therefore

$$ \Delta_p^d E_{j+1/2}^{n+1/2} = \frac{\bar{\mathrm{II}} \; M_{j+1/2}}{G_{j+1/2}^{n+1/2} \left(\rho_{j+1/2}^{n+1} + \rho_{j+1/2}^{n} \right)} \left(\sqrt{\frac{\frac{2}{3}Y^2}{\bar{\mathrm{II}}}} - \frac{\frac{2}{3}Y^2}{\bar{\mathrm{II}}} \right) \qquad \text{A.43} $$

The total deviator stress work is

$$ \Delta^d E_{j+1/2}^{n+1/2} = M_{j+1/2} \, \Delta^d \varepsilon \qquad \text{A.44} $$

and the elastic deviator stress work is simply the difference between equations A.44 and A.43.

A.7 Boundary Conditions

Boundaries and interfaces require no special treatment other than to supply the appropriate quantities on either side of the boundary or interface in the momentum equation A.6.

For a fixed surface quantities σ, q, ρ and ϕ in the mesh outside the fixed surface are set equal to the corresponding quantities in the mesh inside the boundary. Furthermore we set

$$x^n_{J+1} - x^n_J = x^n_J - x^n_{J-1}$$

where J is the boundary index, solving for the appropriate x^n outside the boundary. The acceleration and velocity are then zero and x^{n+1}_J is computed to be equal to x^n_J, as required.

For a free surface, quantities σ, q, ρ and ϕ in the mesh outside the free surface are set equal to zero while x^n outside the boundary is found as above. If a surface pressure is to be introduced, set $\sigma = {}_i p(t)$ where ${}_i p$ is supplied as input either as an analytic fit or in tabular form.

For an internal interface between different materials, no special provisions are required while the materials on either side of the interface are in contact. However, when the stress at the interface, ($\frac{1}{2}$ ($\sigma^{n+1}_{J+1/2} + \sigma^{n+1}_{J-1/2}$) where J is the interface index), exceeds the tensile fracture stress of the bonding, two free surfaces are formed. It is then necessary to store

additional values of x and u for the second surface and apply the free surface conditions when computing the separate accelerations of each surface. If at a later time the surfaces attempt to cross, (i.e. $x_{J-}^{n+1} > x_{J+}^{n+1}$ where $J-$ and $J+$ refer to the left and right hand free surfaces respectively) the positions and velocities of the two surfaces are set equal and the interface is treated as unseparated once more. Subsequent separation of the interface will then occur at zero stress. Actually a small (nonzero) separation stress is used to prevent undesirable separation and contact when the interface stress oscillates about zero. Fractures at the interior of a material are treated in precisely the same way.

A.8 Stability Criterion

The stability criterion is used to compute $\Delta t^{n+3/2}$ used to advance the calculation on the following time cycle. The expression is evaluated for each mesh and the minimum is used for advancing the calculation. Using a backward time centering, the stability criterion becomes

$$\underset{j}{\mathrm{MIN}}\left(\Delta t_{j+1/2}^{n+3/2}\right) = \frac{x_{j+1}^{n+1} - x_{j}^{n+1}}{\left(1+2B_2\right)c_{j+1/2}^{n+1} + 4B_1^2\left|u_{j+1}^{n+1/2} - u_{j}^{n+1/2}\right|} \qquad \text{A.45}$$

In this expression it is tacitly assumed that the velocities at j and $j+1$ will remain the same on the next cycle.

The expression, equation A.45, has been found to be

adequate for most purposes. Experience has shown that even if large velocity discontinuities are introduced initially, as for example at the interface between colliding materials, the computation remains stable and the discontinuity is smoothed to the normal shock width of 3 or 4 meshes within 3 or 4 cycles. However, if an initial pressure discontinuity is introduced, the calculation becomes unstable if equation A.45 is used. A heuristic argument suggests the following explanation. A velocity discontinuity acts immediately to strengthen the stability criterion through the velocity gradient term in the denominator of equation A.45. A pressure discontinuity, however, does not affect the stability criterion until a later cycle when the pressure discontinuity has accelerated the mesh points concerned. A scheme to overcome this limitation has been suggested.[12]

Instead of computing the stability criterion at the conclusion of the calculations for a particular cycle, the stability criterion is computed just after computing the acceleration (equation A.6) but before computing velocity (equation A.7). A forward time centering is used. Moving the entire expression backwards one step in time, we write

$$\Delta t^{n+1/2} = \frac{\Delta x^{n+1}}{(1+2B_2)c^n + 4B_1^2 \left|\Delta u^{n+1/2}\right|} \qquad \text{A.46}$$

where $\Delta x^{n+1} = x_{j+1}^{n+1} - x_j^{n+1}$, etc., and the spatial index is henceforth omitted. The essential difference between equations A.45 and A.46 is in the centering of the Δx and Δu terms. We may

anticipate that Δx^{n+1} and $\Delta u^{n+1/2}$ will differ materially from Δx^{n} and $\Delta u^{n-1/2}$ if the acceleration gradient is high. Such an acceleration gradient would result from a large pressure discontinuity. The sonic velocity c by comparison does not change drastically even with large changes in pressure so that it is sufficient to use c^{n}. At this point in the calculation the velocities and position are not yet available at $n+1$ and $n+1/2$ respectively. However, a good estimate is

$$u_j^{n+1/2} = u_j^{n-1/2} + \Delta t^{n+1/2}\, a_j^{n}$$
$$x_j^{n+1} = x_j^{n} + \Delta t^{n+1/2}\, u_j^{n+1/2} \qquad \text{A.47}$$

since Δt will not be expected to vary too drastically from cycle to cycle.

Inserting equations A.47 into A.46 and investigating limiting solutions for large and small values of Δa^{n} leads to the sufficient condition

$$\underset{j}{MIN}\left(\Delta t_{j+1/2}^{n+1/2}\right) = K\,\Delta x^{n} \Big/ \Big\{ (1+2B_2)\, c_{j+1/2}^{n} + (4B_1^2+1)\left|\Delta u^{n-1/2}\right| + \sqrt{(4B_1^2+1)\,\Delta x^{n}\,\left|\Delta a^{n}\right|}\Big\} \qquad \text{A.48}$$

where $\Delta x^{n} = x_{j+1}^{n} - x_j^{n}$, etc.

A constant K is inserted as a convenience for strengthening the stability criterion artificially if this should be desirable.

Appendix B

Two-Dimensional Finite Difference Equations

B.1 Equations of Motion

Consider discrete points in space formed by the intersection of material coordinate lines distances Δx and Δz apart. Similarly, consider only discrete times finite increments Δt apart. We use three indices to denote values of quantities at the intersection of the ith z material coordinate and j^{th} x material coordinate at the nth time, e.g. $a^{n}_{i,j}$

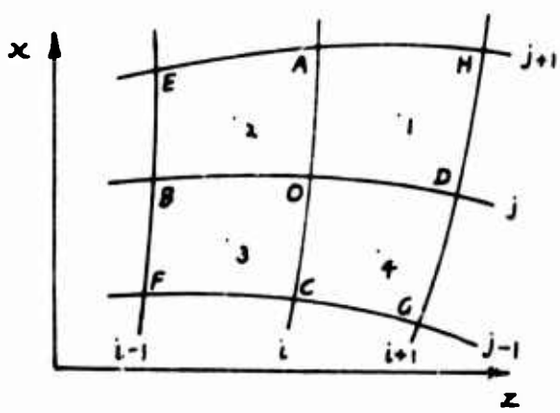

Quantities such as pressure, density, stress, etc. are averaged over the meshes formed by the finite difference grid, and are denoted by $p^{n}_{i+1/2,\, j+1/2}$ etc.

While quantities are indexed in this way in the computer, in writing down the finite difference equations it is more convenient to use the notation shown in the sketch.

Suppose that quantities vary so slowly in time that linear interpolation is justified ,i.e.,

$$\psi_0^{n+1/2} = \frac{1}{2}\left(\psi_0^{n+1} + \psi_0^{n}\right) \qquad \text{B.1}$$

and similarly in space. Such linear interpolation is in accord

with the approximations involved in the finite difference analogs to partial derivatives, correct to second order, i.e. for time derivatives at 0

$$\frac{\partial \Psi}{\partial t} = \frac{\Psi_0^{n+1/2} - \Psi_0^{n-1/2}}{t^{n+1/2} - t^{n-1/2}} \qquad \text{B.2}$$

Finite difference analogs to spatial derivative are obtained by the use of Green's Transformation. For quantities which are averaged over the meshes, Green's Transformation applied to the circuit A B C D gives the gradients at 0

$$\frac{1}{\rho}\frac{\partial \Psi}{\partial x} = \frac{1}{\rho A}\left\{\Psi_1(z_D - z_A) + \Psi_2(z_A - z_B) + \Psi_3(z_B - z_C) + \Psi_4(z_C - z_D)\right\}$$

B.3

$$\frac{1}{\rho}\frac{\partial \Psi}{\partial z} = \frac{-1}{\rho A}\left\{\Psi_1(x_D - x_A) + \Psi_2(x_A - x_B) + \Psi_3(x_B - x_C) + \Psi_4(x_C - x_D)\right\}$$

where A is the area of the quadrilateral A B C D.

The momentum equations, temporarily omitting body forces, become

$$a^x = \frac{1}{\rho}\frac{\partial t^{xx}}{\partial x} + \frac{1}{\rho}\frac{\partial t^{xz}}{\partial z} \quad (\alpha - 1)\frac{t^{xx} - t^{yy}}{\rho x}$$

B.4

$$a^z = \frac{1}{\rho}\frac{\partial t^{xz}}{\partial x} + \frac{1}{\rho}\frac{\partial t^{zz}}{\partial z} + (\alpha - 1)\frac{t^{xz}}{\rho x}$$

where we use equations B.3 to represent the derivative terms and the equations are centered at 0 in space at t^n in time. The term (ρA) appearing in these equations is required at 0, but ρ and A are quantities averaged over the meshes. The simplest solution is to use

$$(\rho A)_0 = \frac{1}{2}\left(\rho_1 A_1 + \rho_2 A_2 + \rho_3 A_3 + \rho_4 A_4\right) \qquad \text{B.5}$$

For cases where areas of severe distortion must be handled as realistically as possible, it is better to use the more accurate but much lengthier relation

$$(\rho A)_0 = \left(\rho_1 A_1' + \rho_2 A_2' + \rho_3 A_3' + \rho_4 A_4'\right)$$

B.6

$$A_1' = \frac{1}{2}\left\{(x_A - x_0)(z_D - z_0) - (x_D - x_0)(z_A - z_0)\right\}$$

is the area of triangle A O D etc. We have used equation B.5.

The last terms on the right of equations B.4 also require interpolation. A variety of interpolation schemes are possible, we have used

$$\frac{\Psi}{\rho x} = \frac{1}{4}\left(\Psi_1 \frac{A_1}{m_1} + \Psi_2 \frac{A_2}{m_2} + \Psi_3 \frac{A_3}{m_3} + \Psi_4 \frac{A_4}{m_4}\right) \qquad \text{B.7}$$

where A and m are the areas and masses of the meshes, defined later. This allows a relatively simple treatment at boundaries.

The velocities and coordinates of cell vertices, using equation B.1, are given by

$$(u^x)_o^{n+1/2} = (u^x)_o^{n-1/2} + \frac{1}{2}\left(\Delta t^{n+1/2} + \Delta t^{n-1/2}\right)(a^x)_o^n$$

B.8

$$(u^z)_o^{n+1/2} = (u^z)_o^{n-1/2} + \frac{1}{2}\left(\Delta t^{n+1/2} + \Delta t^{n-1/2}\right)(a^z)_o^n$$

and

$$x_o^{n+1} = x_o^n + \Delta t^{n+1/2}\,(u^x)_o^{n+1/2}$$

B.9

$$z_o^{n+1} = z_o^n + \Delta t^{n+1/2}\,(u^z)_o^{n+1/2}$$

B.2 Continuity Equation

The continuity equation is taken in integral form. The volume of mesh 3 is given within a factor $(2\pi)^{\alpha-1}$ by

$$V_3^n = A_L\,(x_L)^{\alpha-1} + A_u\,(x_u)^{\alpha-1} \qquad \text{B.10}$$

where A_L and A_u are the areas of the triangles B F C and B O C respectively at time t^n

$$A_L = \frac{1}{2}\left\{(z_c - z_F)(x_B - x_F) - (x_c - x_F)(z_B - z_F)\right\}$$

B.11

$$A_u = \frac{1}{2}\left\{(z_B - z_o)(x_c - x_o) - (z_c - z_o)(x_B - x_o)\right\}$$

and x_L and x_u are the centroids of the triangles B F C and B O C respectively at time t^n

$$x_L = \frac{1}{3}\left(x_B + x_F + x_C\right)$$

B.12

$$x_u = \frac{1}{3}\left(x_B + x_O + x_C\right)$$

The continuity equation is

$$\rho_3^n = \frac{m_3}{V_3^n} \qquad \text{B.13}$$

where m_3 is a constant for each mesh, evaluated at time t^o

$$m_3 = \rho_3^o \left\{ A_L^o \left(x_L^o\right)^{\alpha-1} + A_u^o \left(x_u^o\right)^{\alpha-1} \right\} \qquad \text{B.14}$$

The area of mesh 3 is simply

$$A_3^n = A_L + A_u \qquad \text{B.15}$$

B.3 Stretching and Spin

The components of the stretching deviator and spin tensor are given by

$$^{d}d^{xx} = \frac{\partial u^x}{\partial x} + \frac{1}{3}\frac{\dot{\rho}}{\rho} \qquad {}^{d}d^{zz} = \frac{\partial u^z}{\partial z} + \frac{1}{3}\frac{\dot{\rho}}{\rho}$$

B.16

$$^{d}d^{xz} = \frac{1}{2}\left(\frac{\partial u^x}{\partial z} + \frac{\partial u^z}{\partial x}\right) \qquad w^{xz} = \frac{1}{2}\left(\frac{\partial u^x}{\partial z} - \frac{\partial u^z}{\partial x}\right)$$

Interpolation in both space and time is required in the finite difference analogs to the velocity gradient terms. Applying Green's Theorem to the circuit B F C O and using linear interpolation, we get

$$\frac{\partial \psi}{\partial x} = \frac{1}{2\left(A_3^{n+1} + A_3^{n}\right)} \left\{ \left(\psi_O - \psi_F\right)\left(z_C^{n+1} + z_C^{n} - z_B^{n+1} - z_B^{n}\right) - \left(\psi_C - \psi_B\right)\left(z_O^{n+1} + z_O^{n} - z_F^{n+1} - z_F^{n}\right) \right\}$$

B.17

$$\frac{\partial \psi}{\partial z} = \frac{-1}{2\left(A_3^{n+1} + A_3^{n}\right)} \left\{ \left(\psi_O - \psi_F\right)\left(x_C^{n+1} + x_C^{n} - x_B^{n+1} - x_B^{n}\right) - \left(\psi_C - \psi_B\right)\left(x_O^{n+1} + x_O^{n} - x_F^{n+1} - x_F^{n}\right) \right\}$$

which is centered at 3 and time $t^{n+1/2}$. Also

$$\frac{\dot{\rho}}{\rho} = \frac{2}{\Delta t^{n+1/2}} \left\{ \frac{\rho^{n+1} - \rho^{n}}{\rho^{n+1} + \rho^{n}} \right\} \qquad \text{B.18}$$

B.4 Artificial Viscosity

In order to link the width of shock zones to the mesh size, the artificial viscosity coefficients are set proportional to the mesh size. The bulk viscosity becomes, with all quantities centered at 3

$$q^{n+1} = \rho^{n+1}\left\{ B_2 \sqrt{A^{n+1}}\, c^n \left(\frac{\dot{\rho}}{\rho}\right) + \left[B_1 \sqrt{A^{n+1}} \left(\frac{\dot{\rho}}{\rho}\right)\right]^2 \right\}$$

$$\text{for } \frac{\dot{\rho}}{\rho} > 0 \qquad \text{B.19}$$

$$q^{n+1} = 0 \qquad \text{for } \frac{\dot{\rho}}{\rho} \leq 0$$

The deviator viscous stresses take the form

$$\left({}^d q^{xx}\right)^{n+1} = \rho^{n+1}\left\{ B_4\ \bar{x}\ c^n \left({}^d d^{xx}\right)^{n+1/2} - \left[B_3\ \bar{x}\ \left({}^d d^{xx}\right)^{n+1/2}\right]^2 \right\}$$

$$\left({}^d q^{xz}\right)^{n+1} = \rho^{n+1}\left\{ B_4 \sqrt{\bar{x}\,\bar{z}}\ c^n \left({}^d d^{xz}\right)^{n+1/2} - \left[B_3 \sqrt{\bar{x}\,\bar{z}}\ \left({}^d d^{xz}\right)^{n+1/2}\right]^2 \right\} \qquad \text{B.20}$$

$$\left({}^d q^{zz}\right)^{n+1} = \rho^{n+1}\left\{ B_4\ \bar{z}\ c^n \left({}^d d^{zz}\right)^{n+1/2} - \left[B_3\ \bar{z}\ \left({}^d d^{zz}\right)^{n+1/2}\right]^2 \right\}$$

where

$$\bar{x} = \mathrm{Max}\left(x_o, x_B, x_F, x_c\right) - \mathrm{Min.}\left(x_o, x_B, x_F, x_c\right)$$

$$\bar{z} = \mathrm{Max}\left(z_o, z_B, z_F, z_c\right) - \mathrm{Min.}\left(z_o, z_B, z_F, z_c\right)$$

and ${}^{d}q^{xx}$ and ${}^{d}q^{zz}$ are set equal to zero when the corresponding stretching deviators are positive. These expressions are not properly centered, but since the density and sonic velocity do not change rapidly, this does not introduce any difficulties.

The work done by the viscous stresses in the time interval $\Delta t^{n+1/2}$ is given by

$$\Delta_q^{o}\mathcal{E} = \frac{1}{2}\left(q^{n+1} + q^{n}\right)\left(\frac{\Delta\rho}{\rho^2}\right) \qquad \text{B.21}$$

where $$\frac{\Delta\rho}{\rho^2} = 4\,\frac{\left(\rho^{n+1} - \rho^{n}\right)}{\left(\rho^{n+1} + \rho^{n}\right)^2}$$

for the spherical part, and

$$\begin{aligned}\Delta_q^{d}\mathcal{E} = \frac{\Delta t^{n+1/2}}{\rho^{n+1} + \rho^{n}}\Big\{&\left[\left({}^{d}q^{xx}\right)^{n+1} + \left({}^{d}q^{xx}\right)^{n}\right]\left[2\left({}^{d}d^{xx}\right)^{n+1/2} + \left({}^{d}d^{zz}\right)^{n+1/2}\right] \\ &+ \left[\left({}^{d}q^{zz}\right)^{n+1} + \left({}^{d}q^{zz}\right)^{n}\right]\left[2\left({}^{d}d^{zz}\right)^{n+1/2} + \left({}^{d}d^{xx}\right)^{n+1/2}\right] \\ &+ \left[\left({}^{d}q^{xz}\right)^{n+1} + \left({}^{d}q^{xz}\right)^{n}\right]\left[2\left({}^{d}d^{xz}\right)^{n+1/2}\right]\Big\}\end{aligned} \qquad \text{B.22}$$

for the deviator part.

B.5 Stress Deviator

When the material is elastic, the stress deviators are found from the stretching deviators by the differential equations

$$\frac{\partial\, {}^{d}_{e}t^{xx}}{\partial t} - 2\, w^{xz}\, {}^{d}_{e}t^{xz} = 2\, G\, {}^{d}d^{xx}$$

$$\frac{\partial\, {}^{d}_{e}t^{xz}}{\partial t} + w^{xz}\left({}^{d}_{e}t^{xx} - {}^{d}_{e}t^{zz}\right) = 2\, G\, {}^{d}d^{xz} \qquad \text{B.23}$$

$$\frac{\partial\, {}^{d}_{e}t^{zz}}{\partial t} + 2\, w^{xz}\, {}^{d}_{e}t^{xz} = 2\, G\, {}^{d}d^{zz}$$

The differential terms on the left are set into finite differece form using equation B.2, while the other stress terms on the left must be interpolated to $t^{n+1/2}$ using equation B.1. This leads to the implicit set of equations

$$\left({}^{d}_{e}t^{xx}\right)^{n+1} - \left({}^{d}_{e}t^{xx}\right)^{n} - \Delta t\; w^{xz}\left\{\left({}^{d}_{e}t^{xz}\right)^{n+1} + \left({}^{d}_{e}t^{xz}\right)^{n}\right\} = 2\,\Delta t\; G\, {}^{d}d^{xx}$$

$$\left({}^{d}_{e}t^{xz}\right)^{n+1} - \left({}^{d}_{e}t^{xz}\right)^{n} + \frac{1}{2}\Delta t\; w^{xz}\left\{\left({}^{d}_{e}t^{xx}\right)^{n+1} + \left({}^{d}_{e}t^{xx}\right)^{n} - \left({}^{d}_{e}t^{zz}\right)^{n+1} - \left({}^{d}_{e}t^{zz}\right)^{n}\right\} \qquad \text{B.24}$$

$$= 2\,\Delta t\; G\, {}^{d}d^{xz}$$

$$\left({}^{d}_{e}t^{zz}\right)^{n+1} - \left({}^{d}_{e}t^{zz}\right)^{n} + \Delta t\; w^{xz}\left\{\left({}^{d}_{e}t^{xz}\right)^{n+1} + \left({}^{d}_{e}t^{xz}\right)^{n}\right\} = 2\,\Delta t\; G\, {}^{d}d^{zz}$$

where all quantities except stresses are centered at $t^{n+1/2}$

If we choose the time increment $\Delta t^{n+1/2}$ sufficiently small so that

$$\left(\Delta t^{n+1/2} \; w^{xz\;n+1/2}\right)^2 << 1 \qquad \text{B.25}$$

then these equations may be expressed in a relatively simple explicit form. The condition B.25 implies that the rotation from t^n to t^{n+1} is small. Since the spin is the angular velocity, the rotation in time $\Delta t^{n+1/2}$ is

$$\Delta\phi = \Delta t^{n+1/2} \; w^{xz\;n+1/2} \qquad \text{B.26}$$

Defining

$$\Delta_e^d t^{xx} = 2\,\Delta t^{n+1/2}\, G^{n+1/2} \left({}^d d^{xx}\right)^{n+1/2}$$

$$\Delta_e^d t^{xz} = 2\,\Delta t^{n+1/2}\, G^{n+1/2} \left({}^d d^{xz}\right)^{n+1/2} \qquad \text{B.27}$$

$$\Delta_e^d t^{zz} = 2\,\Delta t^{n+1/2}\, G^{n+1/2} \left({}^d d^{zz}\right)^{n+1/2}$$

where we take the shear modulus as a function of compression η

$$G = g_0 \left\{ 1 + g_1 \eta + g_2 \eta^2 + \cdots \right\} \qquad \text{B.28}$$

we find that equations B.24 solved for the stress deviators at time t^{n+1} become approximately

$$ {}_e^d t^{xx} = \left({}_e^d t^{xx}\right)^n + \Delta {}_e^d t^{xx} + 2\Delta\phi \left\{\left({}_e^d t^{xz}\right)^n + \tfrac{1}{2}\Delta {}_e^d t^{xz}\right\} $$

$$ {}_e^d t^{zz} = \left({}_e^d t^{zz}\right)^n + \Delta {}_e^d t^{zz} - 2\Delta\phi \left\{\left({}_e^d t^{xz}\right)^n + \tfrac{1}{2}\Delta {}_e^d t^{xz}\right\} \qquad \text{B.29} $$

$$ {}_e^d t^{xz} = \left({}_e^d t^{xz}\right)^n + \Delta {}_e^d t^{xz} - \Delta\phi \left\{\left({}_e^d t^{xx}\right)^n + \tfrac{1}{2}\Delta {}_e^d t^{xx} - \left({}_e^d t^{zz}\right)^n - \tfrac{1}{2}\Delta {}_e^d t^{zz}\right\} $$

It is readily seen that in each equation the second term on the right represents the stress increment due to stretching, while the last term represents that due to a small rotation.

These equations are, of course, only valid when the material remains elastic. When the material is plastic, only the elastic stretching should appear in the above equations, and it is necessary to solve the set of simultaneous equations for the unknown stress components and proportionality factor ϕ A method of forward differencing used by Wilkins and Giroux,[3] and Maenchen and Sack[4] is used. Consider an elastic stress state at time t^n. If we were to transform to principal coordinates, this stress state could be plotted in the π plane representation as point 1, say (see diagram on next page).

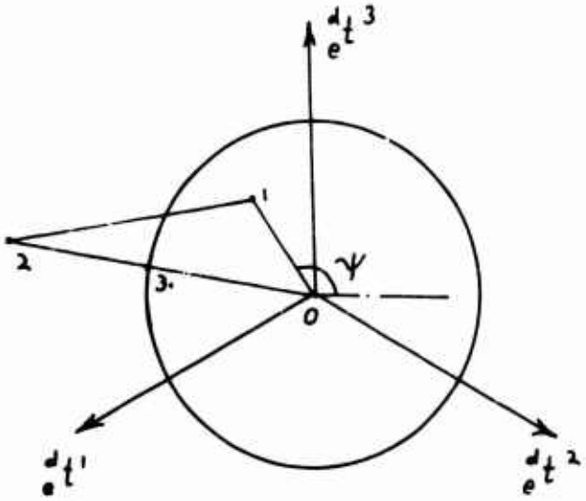

Equations B.26 to B.28 are used to compute a new elastic stress state at t^{n+1}. Transforming to a new set of principal coordinates (which are in general rotated with respect to the previous ones) we can again represent this state in the π plane. The second moment is

$$\bar{\Pi} = 2\left\{\left({}^{d}_{e}t^{xx}\right)^{2} + \left({}^{d}_{e}t^{xz}\right)^{2} + \left({}^{d}_{e}t^{zz}\right)^{2} + \left({}^{d}_{e}t^{xx}\right)\left({}^{d}_{e}t^{zz}\right)\right\} \qquad \text{B.30}$$

Then if $\bar{\Pi} \leq \frac{2}{3} Y^{2}$

Use

$$\left({}^{d}_{e}t^{xx}\right)^{n+1} = {}^{d}_{e}t^{xx}$$

$$\left({}^{d}_{e}t^{xz}\right)^{n+1} = {}^{d}_{e}t^{xz} \qquad \text{B.31}$$

$$\left({}^{d}_{e}t^{zz}\right)^{n+1} = {}^{d}_{e}t^{zz}$$

since the material is still elastic.

However if $\bar{\Pi} > \frac{2}{3} Y^{2}$

the material has become plastic as shown in the diagram. Approximately the correct yield stress is achieved by using

$$\left({}^{d}_{e}t^{xx}\right)^{n+1} = \sqrt{\frac{\frac{2}{3}Y^2}{\bar{\bar{II}}}}\ {}^{d}_{e}t^{xx}$$

$$\left({}^{d}_{e}t^{xz}\right)^{n+1} = \sqrt{\frac{\frac{2}{3}Y^2}{\bar{\bar{II}}}}\ {}^{d}_{e}t^{xz} \qquad \text{B.32}$$

$$\left({}^{d}_{e}t^{zz}\right)^{n+1} = \sqrt{\frac{\frac{2}{3}Y^2}{\bar{\bar{II}}}}\ {}^{d}_{e}t^{zz}$$

which in effect computes the stress state at point 3 on the yield surface on a radius vector from state 2. The proceedure is only valid when the change in Lode's angle is small. Due to the rotation of the principal axes, the principal stress components must be found before Lode's angle may be determined. We have for principal stress deviators

$${}^{d}_{e}t^{a} = \frac{1}{2}\left\{{}^{d}_{e}t^{xx} + {}^{d}_{e}t^{zz} \pm \sqrt{\left({}^{d}_{e}t^{xx} - {}^{d}_{e}t^{zz}\right)^2 + 4\left({}^{d}_{e}t^{xz}\right)^2}\right\} \qquad \text{B.33}$$

where $a = 1, 2$ respectively when the upper or lower sign is used. The angles of the principal axes with respect to the x coordinate axis are

$$\theta_a = \arctan \frac{{}^{d}_{e}t^{xx} - {}^{d}_{e}t^{a}}{{}^{d}_{e}t^{xz}} \qquad \text{B.34}$$

and Lode's angle is given by

$$\psi = \arctan \sqrt{3} \; \frac{{}^{d}_{e}t^{1} - {}^{d}_{e}t^{2}}{{}^{d}_{e}t^{1} + {}^{d}_{e}t^{2}} \qquad \text{B.35}$$

Note that principal components and directions are not required except optionally for diagnostic purposes.

Finally the deviator stress work is given by

$$\Delta^{d}\mathcal{E} = \frac{\Delta t^{n+1/2}}{\rho^{n+1} + \rho^{n}} \Big\{ \Big[\big({}^{d}_{e}t^{xx}\big)^{n+1} + \big({}^{d}_{e}t^{xx}\big)^{n} \Big] \Big[2\big({}^{d}d^{xx}\big)^{n+1/2} + \big({}^{d}d^{zz}\big)^{n+1/2} \Big]$$

$$+ \Big[\big({}^{d}_{e}t^{zz}\big)^{n+1} + \big({}^{d}_{e}t^{zz}\big)^{n} \Big] \Big[2\big({}^{d}d^{zz}\big)^{n+1/2} + \big({}^{d}d^{xx}\big)^{n+1/2} \Big] \qquad \text{B.36}$$

$$+ \Big[\big({}^{d}_{e}t^{xz}\big)^{n+1} + \big({}^{d}_{e}t^{xz}\big)^{n} \Big] \Big[\; 2\big({}^{d}d^{xz}\big)^{n+1/2} \; \Big] \Big\}$$

B.6 Pressure

The pressure is taken as a function of the thermodynamic state in the form

$${}_{e}p = f_1(\rho) + \mathcal{E} \cdot f_2(\rho) \qquad \text{B.37}$$

where in terms of $\eta = (\rho - \rho_0)/\rho$

$$f_1 = k_0 \eta \left\{ 1 + k_1 \eta + k_2 \eta^2 + \cdots \right\}$$

$$f_2 = h_0 \left\{ 1 + h_1 \eta + h_2 \eta^2 + \cdots \right\}$$

while the energy equation in finite difference form is

$$\mathcal{E}^{n+1} + \mathcal{E}^{n} = \frac{1}{2}\left({}_{e}p^{n+1} + {}_{e}p^{n}\right)\frac{\Delta\rho}{\rho^{2}} + \Delta_{q}^{o}\mathcal{E} + \Delta_{q}^{d}\mathcal{E} + \Delta^{d}\mathcal{E} \qquad \text{B.38}$$

where $\Delta\rho/\rho^2$ is given following equation B.21. Solving equation B.37 and B.38 for $\mathcal{E}^{n+1}$

$$\mathcal{E}^{n+1} = \frac{\mathcal{E}^{n} + \frac{1}{2}\left(f_{1}^{n+1} + {}_{e}p^{n}\right)\frac{\Delta\rho}{\rho^{2}} + \Delta_{q}^{o}\mathcal{E} + \Delta_{q}^{d}\mathcal{E} + \Delta^{d}\mathcal{E}}{1 - \frac{1}{2}f_{2}^{n+1}\frac{\Delta\rho}{\rho^{2}}} \qquad \text{B.39}$$

The pressure can then be found from equation B.37. Then the total stress components are given by

$$\begin{aligned} t^{xx} &= {}_{e}^{d}t^{xx} + {}^{d}q^{xx} - \left({}_{e}p + q\right) \\ t^{zz} &= {}_{e}^{d}t^{zz} + {}^{d}q^{zz} - \left({}_{e}p + q\right) \\ t^{xz} &= {}_{e}^{d}t^{xz} + {}^{d}q^{xz} \end{aligned} \qquad \text{B.40}$$

$$t^{xx} - t^{yy} = 2\,{}_{e}^{d}t^{xx} + {}_{e}^{d}t^{zz} + 2\,{}^{d}q^{xx} + {}^{d}q^{zz}$$

The bulk modulus K is obtained by differentiating equation B.37 with respect to ρ at constant entropy. Assuming that Poisson's ratio remains near 1/3, a good expression for the elastic sound speed is $c = \sqrt{1.5\,K/\rho}$ whence

$$\left(c^{n+1}\right)^{2} = \frac{1.5}{\rho^{n+1}}\left\{\left(\rho\frac{\partial f_{1}}{\partial\rho}\right)^{n+1} + \mathcal{E}^{n+1}\left(\rho\frac{\partial f_{2}}{\partial\rho}\right)^{n+1} + \frac{f_{2}^{n+1}\,{}_{e}p^{n+1}}{\rho^{n+1}}\right\} \qquad \text{B.41}$$

where

$$\rho \frac{\partial f_1}{\partial \rho} = k_0 \left\{ 1 + 2k_1 \eta + 3k_2 \eta^2 + \cdots \right\} (1-\eta)$$

$$\rho \frac{\partial f_2}{\partial \rho} = h_0 \left\{ h_1 + 2h_2 \eta + 3h_3 \eta^2 + \cdots \right\} (1-\eta)$$

B.7 Energy Checks

It is often desirable to study momentum and energy of individual meshes, or summed over portions or the whole of the material in the problem. The finite difference expressions below are collected for convenience, and are incorporated in a special subroutine only when required for diagnostic purposes.

The mass of mesh 3 is given by

$$M_3 = (2\pi)^{\alpha-1} m_3 \qquad \text{B.42}$$

Thus the momentum components in mesh 3 are approximately

$$H^x{}_3^{n+1/2} = M_3 \; u^x{}_3^{n+1/2}$$

$$H^z{}_3^{n+1/2} = M_3 \; u^z{}_3^{n+1/2} \qquad \text{B.43}$$

while the kinetic energy components are

$$K^x{}_3^{n+1/2} = \frac{1}{2} M_3 \left(u^x{}_3^{n+1/2} \right)^2$$

$$K^z{}_3^{n+1/2} = \frac{1}{2} M_3 \left(u^z{}_3^{n+1/2} \right)^2 \qquad \text{B.44}$$

where in equations B.43 and B.44 we interpolate the velocity components as

$$u_3 = \frac{1}{4}\left(u_A + u_C + u_D + u_H \right) \qquad \text{B.45}$$

The internal energy is

$$E_3^{n+1/2} = \frac{1}{2} M_3 \left(\mathcal{E}_3^{n+1} + \mathcal{E}_3^{n} \right) \qquad \text{B.46}$$

It is useful to sum kinetic and internal energy over the material. Then if energy is conserved

$$\sum_{i,j} \left(K^x + K^z + E \right)^{n+1/2} - \sum_{i,j} \left(K^x + K^z + E \right)^{n-1/2} = \mathcal{W}^{n+1/2} + \mathcal{Q}^{n+1/2} \qquad \text{B.47}$$

where $\mathcal{W}^{n+1/2}$ is the surface work done from time t^n to time t^{n+1} (for example by a surface pressure) and $\mathcal{Q}^{n+1/2}$ is the nonmechanical energy addition in this time interval (for example, chemical energy in an explosive). This provides a very useful check on the calculation.

It is very simple to find the energy dissipation in various modes during the time interval t^n to t^{n+1}. The spherical elastic stress work is

$$\Delta\, {}_e^{\circ}E_3^{n+1/2} = \frac{1}{2} M_3 \left({}_eP_3^{n+1} + {}_eP_3^{n} \right) \frac{\Delta\rho}{\rho^2} \qquad \text{B.48}$$

while the spherical and deviator viscous stress work are given by

$$\Delta_q^{\circ} E_3^{n+1/2} = M_3 \, \Delta_q^{\circ} \mathcal{E}$$

$$\Delta_q^{d} E_3^{n+1/2} = M_3 \, \Delta_q^{d} \mathcal{E} \qquad \text{B.49}$$

The plastic stress work is, as for the one dimensional case,

$$\Delta_p^{d} E_3^{n+1/2} = \frac{\bar{\Pi} \; M_3}{G_3^{n+1/2}\left(\rho_3^{n+1} + \rho_3^{n}\right)} \left\{ \sqrt{\frac{\frac{2}{3} Y^2}{\bar{\Pi}}} - \frac{\frac{2}{3} Y^2}{\bar{\Pi}} \right\} \qquad \text{B.50}$$

The total deviator stress work is

$$\Delta^{d} E_3^{n+1/2} = M_3 \, \Delta^{d} \mathcal{E} \qquad \text{B.51}$$

and the elastic deviator stress work is simply the difference between equations B. 51 and B.50.

B.8 Boundary Conditions

Boundaries and interfaces require no special treatment other than to supply the appropriate quantities in the meshes surrounding a boundary or interface point in the momentum equations B.4.

For a fixed surface along which the material may slide, normal stresses t^{xx} and t^{zz}, densities ρ, areas and masses A and m in the meshes outside the boundary are set equal to the values in the corresponding meshes inside the boundary, while the shear stresses t^{xz} are reflected antisymmetrically. It is also necessary to supply the coordinates of mesh vertices outside

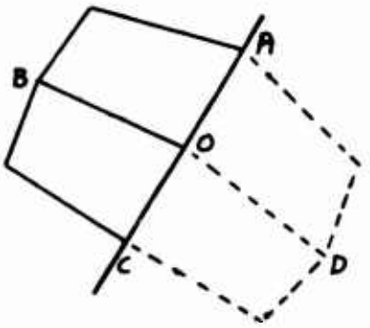

the boundary. If A C is the boundary, we require coordinates of point D outside the boundary which is a reflection of point B inside the boundary. The equations are

$$x_D = \frac{1}{A}\left\{ x_{\overline{AC}}^2\, x_B + z_{\overline{AC}}^2 \left(x_A - x_B + x_C\right) - x_{\overline{AC}}\, z_{\overline{AC}} \left(z_A - 2 z_B + z_C\right) \right\}$$

B.52

$$z_D = \frac{1}{A}\left\{ z_{\overline{AC}}^2\, z_B + x_{\overline{AC}}^2 \left(z_A - z_B + z_C\right) - z_{\overline{AC}}\, x_{\overline{AC}} \left(x_A - 2 x_B + x_C\right) \right\}$$

where

$$x_{\overline{AC}} = x_A - x_C \;, \quad z_{\overline{AC}} = z_A - z_C \;, \quad A = x_{\overline{AC}}^2 + z_{\overline{AC}}^2$$

For a free surface, the stresses and densities are set equal to zero in the meshes outside the boundary. To prevent difficulties with zeros in the denominators of terms in equation B.7 , A , m, x, and z for the cells outside the boundary are treated as for a fixed surface. If a surface pressure is to be introduced, set $t^{xx} = t^{zz} = -{}_i p(t)$ where ${}_i p(t)$ is supplied as input either as an analytic fit or in tabular form.

Corners require no special consideration, except that

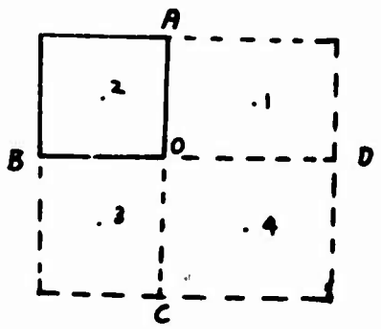

x_o , z_o are used in place of x_c, z_c to find the position of point D outside the boundary (and similarly for point C). Values in the corner mesh outside the boundaries (mesh 4 in the diagram) may be obtained

either by applying the proper boundary condition along A O to find values in mesh 1, and subsequently applying the proper boundary condition along B D to find values in meshes 3 and 4, or by applying the proper boundary conditions along B O to find values in mesh 3, subsequently applying the proper boundary conditions along A C to find values in meshes 1 and 4. In either case identical results are obtained. Reentrant corners are generally formed by the meeting of two free surfaces, and it is unnecessary to find values of x and z at points C and D (in the diagram) by equation B.52.

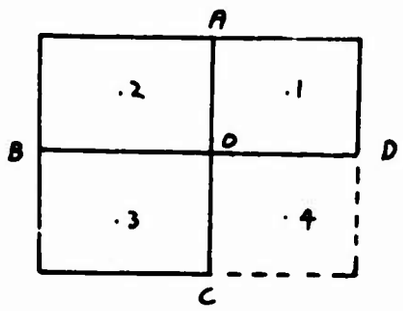

However no harm is done if equation B.52 is used, and it is more convenient to retain complete generality at all boundary points.

Interfaces between different materials require no special provisions while the materials remain in contact without sliding. Sliding interfaces and separated interfaces require individual treatment, as do internal fractures. These can be incorporated as required.

B.9 Stability Criterion

The stability criterion is used to compute $\Delta t^{n+3/2}$ which is used to advance the calculation on the following time cycle. Using a backward time centering

$$\underset{J}{\mathrm{MIN}}\left(\Delta t^{n+1/2}\right) = \frac{K\sqrt{A^{n+1}}}{\left(1+2B_4\right)c^{n+1} + 4B_3^{\,2}\sqrt{A^{n+1}}\,\left|\left(\dot{\rho}/\rho\right)^{n+1/2}\right|} \qquad \text{B.53}$$

where the minimum is taken over all meshes. A constant K is inserted as a convenience for strengthening the stability criterion artificially if this should be desirable.

Appendix C

Evaluation of Constitutive Equation Constants

The constitutive equations appearing in Section III have been specialised to specific classes of materials, by making assumptions that the materials are perfect fluids or compressible elastic-perfectly plastic solids. The assumption was made (equation 3.6) that the spherical part took the form

$$p = f_1(\rho) + \varepsilon . f_2(\rho) \qquad \text{C.1}$$

where f_1 and f_2 were left as arbitrary functions, although it was intimated that power series expansions could be used. It is not necessary to limit ourselves to the form of equation C.1, and it is quite feasible to use a more general expression

$$p = f(\rho, \varepsilon) \qquad \text{C.2}$$

although the convenient explicit finite difference scheme for finding the internal energy and pressure outlined in Apendices A and B, which is made possible by the form of equation C.1, must be abandoned, and replaced by an iteration scheme. It was found that an iteration scheme often required more than three iterations to assure accuracy, and it has been deemed preferable to express the spherical relation in the form of equation C.1 wherever possible.

The present appendix is concerned with evaluating some special forms of the functions f_1 and f_2 for some restricted cases,

and is thus much more specialised and restricted than the material in the body of the report. The functions are developed for a solid or fluid from measured Hugoniot data using the Mie-Grueneisen equation. For a gas, the functions are developed from measured Chapman-Jouguet isentropes by somewhat similar means. These approaches should be reasonably accurate up to moderately high pressures, such as those encountered in solid-explosive systems. Other means of evaluating the spherical constitutive equation could, of course, be substituted.

C.1 Solid or Fluid

Hugoniots (loci of states attainable in a single shock compression from the normal state) have been evaluated for a wide variety of materials from experimental determinations of shock and particle velocities[13] by means of the Rankine-Hugoniot relations

$$\eta = \frac{[u]}{[U]}$$

$$[p] = \rho_0 [u][U] \qquad \text{C.3}$$

$$[\mathcal{E}] = \frac{[p]\eta}{2\rho_0}$$

where $\eta = (\rho - \rho_0)/\rho$, $(\ )_0$ refers to the state ahead of the shock, $[\ ]$ refers to the jump in variables across the

shock, and U is the shock velocity ($[U] = U - u_o$). Results are often fitted to the power series.

$$p_H = k_o' \eta \left(1 + k_1' \eta + k_2' \eta^2 + \cdots \right) \qquad \text{C.4}$$

where the normal state is taken at $p_o = 0$.

For moderate compressions it is found experimentally[14] that the shock velocity is a linear function of particle velocity

$$U = c + s\,u \qquad \text{C.5}$$

where c is the bulk sound speed and s is a parameter (the material ahead of the shock is taken to be stationary, $u_o = 0$) so that equations C.3 a and b become

$$p_H = \frac{\rho_o c^2 \eta}{(1 - s\eta)^2} \qquad \text{C.6}$$

Expanding to the form of equation C.4, we obtain immediately

$$k_o' = \rho_o c^2 \qquad k_1' = 2s \qquad k_2' = 3s^2 \qquad \text{C.7}$$

Terms in k_2' and higher need not be retained since the linear relation, equation C.5, is not valid except when η is small. (This follows directly from equation C.6, for we note that $p \to \infty$ when $\eta \to 1/s$, a physically unreasonable situation. Since s is generally found to lie between 1 and 2 for most materials, equations C.6 and C.7 must be limited to compressions of perhaps 0.1.)

Note that the coefficient k_o' represents the

adiabatic bulk modulus of the material at zero pressure.

The Murnaghan equation

$$p_H = A\left\{\left(\frac{\rho}{\rho_0}\right)^{\xi} - 1\right\} \qquad \text{C.8}$$

has occasionally been used to fit experimental shock Hugoniots.[15] Expanding to the form of equation C.7 we obtain

$$k_0' = A\xi \qquad k_1' = \tfrac{1}{2}(\xi+1) \qquad k_2' = \tfrac{1}{6}(\xi+1)(\xi+2) \qquad \text{C.9}$$

where again higher order terms need not be retained.

It might be noted that the assumption of a linear Hookean material with Lamé constants λ and μ leads via finite strain theory to a relation between the pressure and volumetric strain[16]

$$p = -(1-2\epsilon)^{5/2}\, 3\epsilon\left(\lambda + \tfrac{2}{3}\mu\right) \qquad \text{C.10}$$

where $\rho = \rho_0(1-2\epsilon)^{3/2}$

which is easily expanded into the form of equation C.7, whence

$$k_0' = \left(\lambda + \tfrac{2}{3}\mu\right) \qquad k_1' = 5/2 \qquad k_2' = 235/54 \qquad \text{C.11}$$

The above relations provide a direct means of comparison of experimental data fitted to the different empirical expressions, and allow the data to be easily put into the form of equation C.7, which is used as a basis for the following discussion.

The Hugoniot data is generalised by making the assumption that the pressure offset of a state from the Hugoniot is proportional to the energy density offset[13]

$$(p - p_H) = \gamma \rho \, (\mathcal{E} - \mathcal{E}_H) \qquad \text{C.12}$$

where γ is the Grüneisen ratio. $p_H(\rho)$ and $\mathcal{E}_H(\rho)$ are available from equations C.7 and C.3c, while $\gamma(\rho)$ has been evaluated approximately for numerous metals in the form[13]

$$\gamma = \gamma_0 \, (1 + \gamma_1 \eta + \gamma_2 \eta^2 + \gamma_3 \eta^3 + \cdots) \qquad \text{C.13}$$

The thermodynamic relation at zero pressure should be noted

$$\gamma_0 = \frac{k_0 \alpha}{\rho_0 c_p} \qquad \text{C.14}$$

where α is the volumetric thermal expansion coefficient and c_p is the specific heat at constant pressure. For moderate compressions, it seems to be sufficiently accurate to take $\gamma = \gamma_0$ constant.

Equation C.12 can easily be put into the form of equation C.1, whence

$$f_1 = p_H - \gamma \rho \mathcal{E}_H$$

$$f_2 = \gamma \rho \qquad \text{C.15}$$

Inserting equations C.3 and C.13 for p_H, $\mathcal{E}_H$ and γ allows these functions to be put in the form of power series in η

$$f_1 = k_0 \eta \, (1 + k_1 \eta + k_2 \eta^2 + k_3 \eta^3 + \cdots) \qquad \text{C.16}$$

$$f_2 = h_0 \, (1 + h_1 \eta + h_2 \eta^2 + h_3 \eta^3 + \cdots)$$

where

$$k_0 = k_0' \qquad h_0 = \rho_0 \gamma_0$$

$$k_1 = k_1' - \tfrac{1}{2}\gamma_0 \qquad h_1 = 1 + \gamma_1$$

$$k_2 = k_2' - \tfrac{1}{2}\gamma_0 (h_1 + k_1') \qquad h_2 = 1 + \gamma_1 + \gamma_2$$

$$k_3 = k_3' - \tfrac{1}{2}\gamma_0 (h_2 + h_1 k_1' + k_2') \qquad h_3 = 1 + \gamma_1 + \gamma_2 + \gamma_3$$

etc.

For a solid, the deviator part of the constitutive equation depends on the shear modulus which was also expressed as a power series in the compression. The variation in shear modulus is considered in another report.[17] Since velocity of longitudinal elastic waves is given by

$$c_e = \sqrt{(K + \tfrac{4}{3} G)/\rho} \qquad \text{C.17}$$

the error in elastic wave velocity due to an error in G is only

$$\frac{\Delta c_e}{c_e} = \frac{\Delta G}{G} \Big/ \left(\frac{3}{2} \frac{K}{G} + 2 \right) \qquad \text{C.18}$$

or for Poisson's ratio near $\frac{1}{3}$, $\frac{\Delta c}{c} \propto \frac{1}{6} \frac{\Delta G}{G}$. Also, the error in stress deviator is proportional to the error in G, but in the presence of a pressure component, the error in the total stress is smaller than this. For moderate compressions, it is therefore probably sufficient to take G as a constant. Jones has investigated the variation in G on the basis of several assumptions, and has discussed means of finding higher order terms in a series expansion for G.[17]

C.2 Nonideal Gas

The spherical constitutive equation for a gas must take a different form from that for a solid since in the latter the density is nonzero at zero pressure, and pressures may become negative (or tensile).

We consider only a gas in which a known isentrope may be fitted by a polytropic law

$$p_i = A \rho^{\beta} \qquad \text{C.19}$$

where $A = p_1 \rho_1^{-\beta}$ is a constant evaluated at a known point. This approach is applicable to a simple description of gaseous explosion products.[18] Chapman-Jouguet isentropes have been measured for some explosives, p_1 and ρ_1 are then the CJ pressure and density respectively.

The isentrope given by equation C.19 can be expanded to cover nearby states by again assuming that the pressure offset is proportional to the energy density offset.[17]

$$(p - p_i) = \gamma \rho \, (\mathcal{E} - \mathcal{E}_i) \qquad \text{C.20}$$

In this case $\mathcal{E}_i$ is the internal energy on the isentrope, given by

$$\mathcal{E}_i = -\int p_i \, d\left(\frac{1}{\rho}\right) = \frac{p_i}{\rho(\beta - 1)} \qquad \text{C.21}$$

Equation C.20 can then be put into the form

$$p = f_1 + \mathcal{E} . f_2 \qquad \text{C.22}$$

where

$$f_1 = p_i - \gamma \rho \mathcal{E}_i = \mathcal{K} \rho^{\beta}$$

$$f_2 = \gamma \rho$$

where we have substituted from equations C.19 and C.21, and where

$$\mathcal{K} = p_1 \rho_1^{-\gamma} \left(1 - \frac{\gamma}{\beta - 1} \right) \qquad \text{C.23}$$

REFERENCES

1. Herrmann, W., and Jones, A.H. "Correlation of Hypervelocity Impact Data." Proceedings of the Fifth Hypervelocity Impact Symposium. 30 October - 1 November 1961, Denver, Colorado.

2. Curran, D. R. "Nonhydrodynamic Attenuation of Shock Waves in Aluminum." Journal of Applied Physics, Vol. 34, p. 2677, 1963.

3. Wilkins, M. L., and Giroux, R. Calculation of Elastic-Plastic Flow. UCRL-7322, April 1963.

4. Maenchen, G., and Sack, S. The Tensor Code. UCRL 7316, April 1963.

5. Truesdell, C., and Toupin, R. A. "The Classical Field Theories." Encyclopedia of Physics. Ed. S. Flügge, Vol. 3/1, pp. 226-793, 1960.

6. Von Neumann, and Richtmyer. "A Method for the Numerical Calculation of Hydrodynamic Shocks." Journal of Applied Physics, Vol. 21, p. 232, 1950.

7. Thomas, T. Y. Plastic Flow and Fracture in Solids. Academic Press, 1961.

8. Hill, R. The Mathematical Theory of Plasticity. Oxford University Press, 1950.

9. Landshoff, R. A Numberical Method for Treating Fluid Flows in the Presence of Shocks. LA 1930, January 1955.

10. Herrmann, W. Comparison of Finite Difference Expressions Used in Lagrangian Fluid Flow Calculations. AFWL TR 64-104.

11. Kolsky, H. G. A Method for the Numerical Solution of Transient Hydrodynamic Shock Problems in Two Space Dimensions. LA 1867, September 1954.

12. Lemcke, B. Private communication.

13. Rice, M. H., McQueen, R. G., and Walsh, J. M. "Compression of Solids by Strong Shock Waves." Solid State Physics, Vol. 6, pp. 1 - 63, 1958.

14. McQueen, R. G., and Marsh, S. P. "Equation of State for Nineteen Metallic Elements from Shock Wave Measurements to Two Megabars." Journal of Applied Physics, Vol. 31, p. 1253, 1960.

15. Fowles, G. R. "Attenuation of the Shock Wave Produced in a Solid by a Flying Plate." Journal of Applied Physics, Vol. 31, p. 655, 1960.

16. Birch, F. "The Effect of Pressure Upon the Elastic Parameters of Isotropic Solids, According to Murnaghan's Theory of Finite Strains." Journal of Applied Physics, Vol. 9, p. 279, 1938.

17. Jones, A. H. Variation of Elastic Moduli. AFWL TR 64-103.

18. Fickett, W., and Wood, W. W. "A Detonation Product Equation of State Obtained from Hydrodynamic Data." The Physics of Fluids, Vol. 1, p. 528, 1958.

19. Calvit, H. H., and Davids, N. Spherical Shock Waves in Solids. Penn. State University, Technical Report No. 2, July 1963.

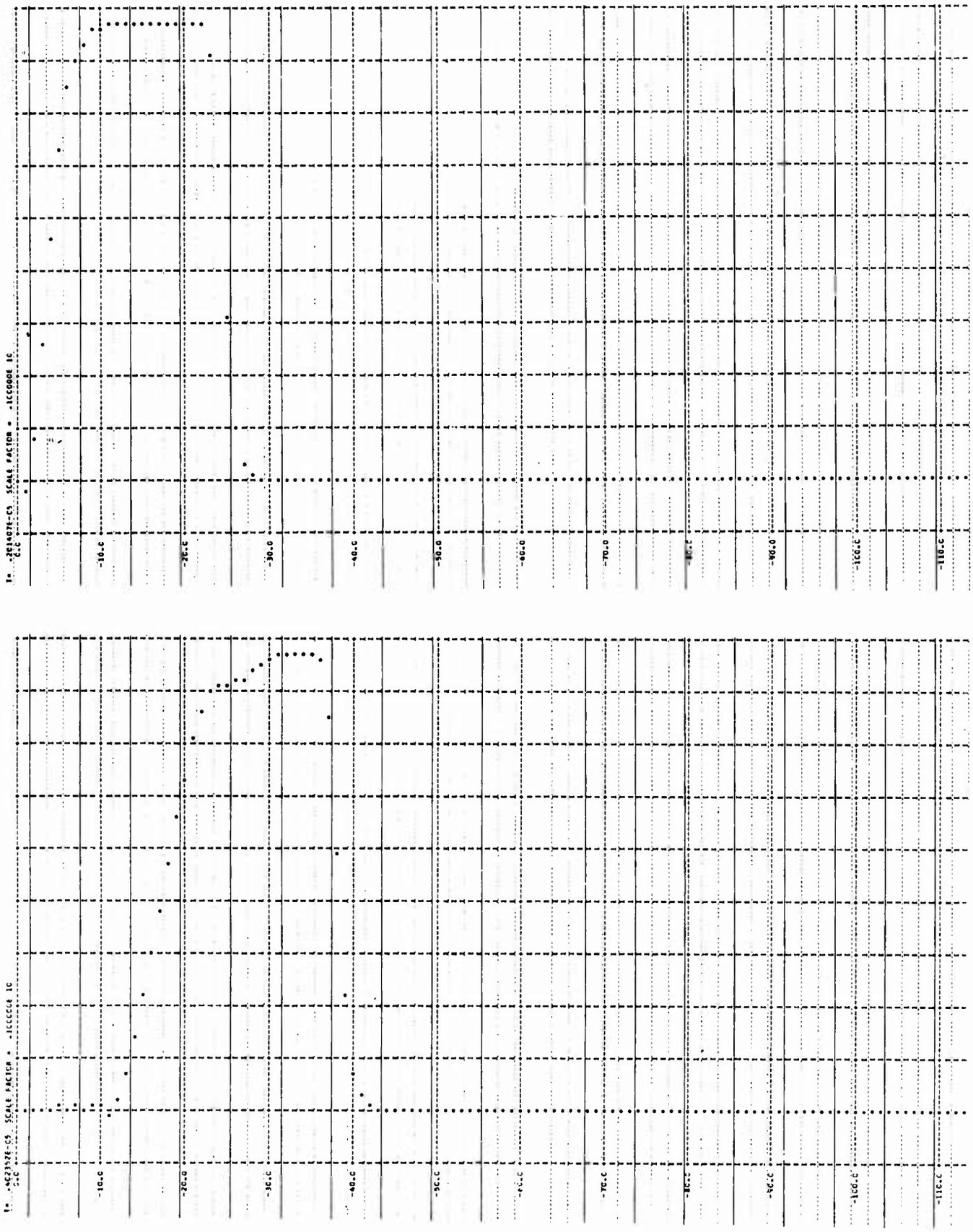

Figure 1. Elastic-Plastic Plate Impact at Initial Velocity 1.9 km/sec. Stress Profiles at 2 and 4 micro-seconds

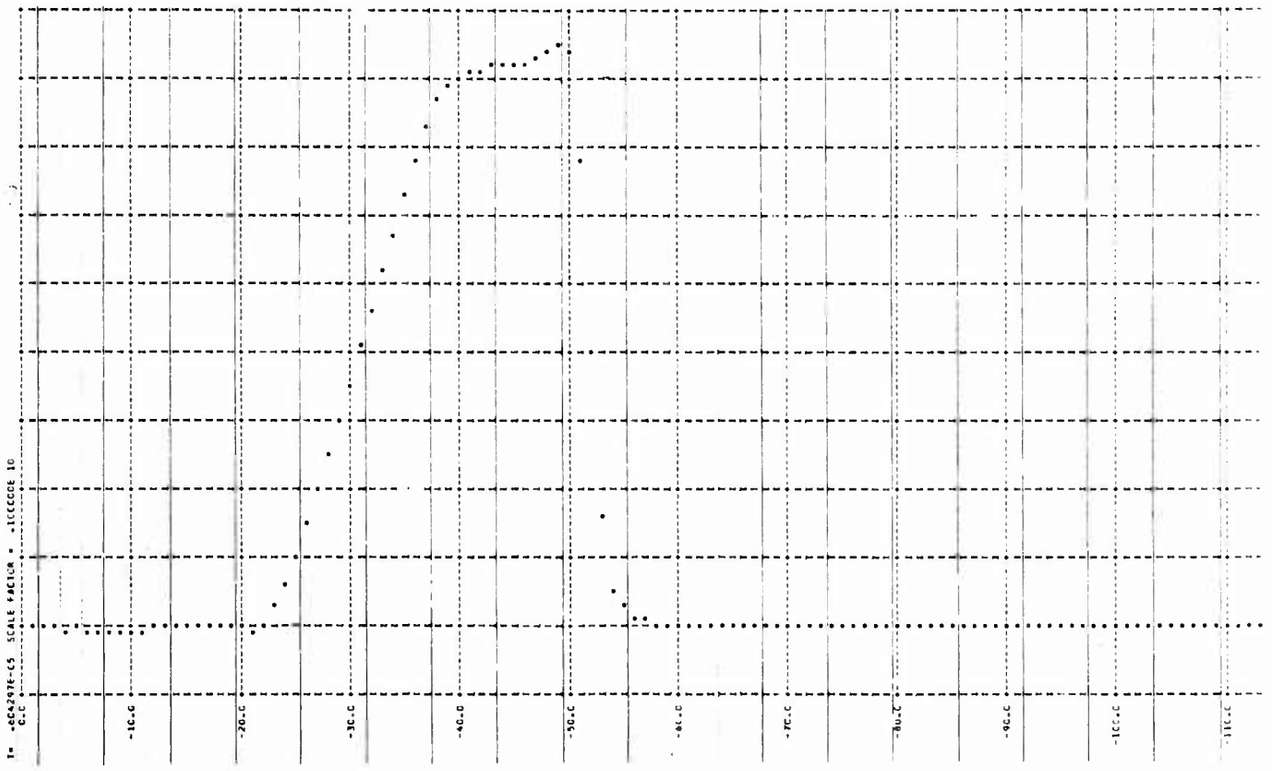

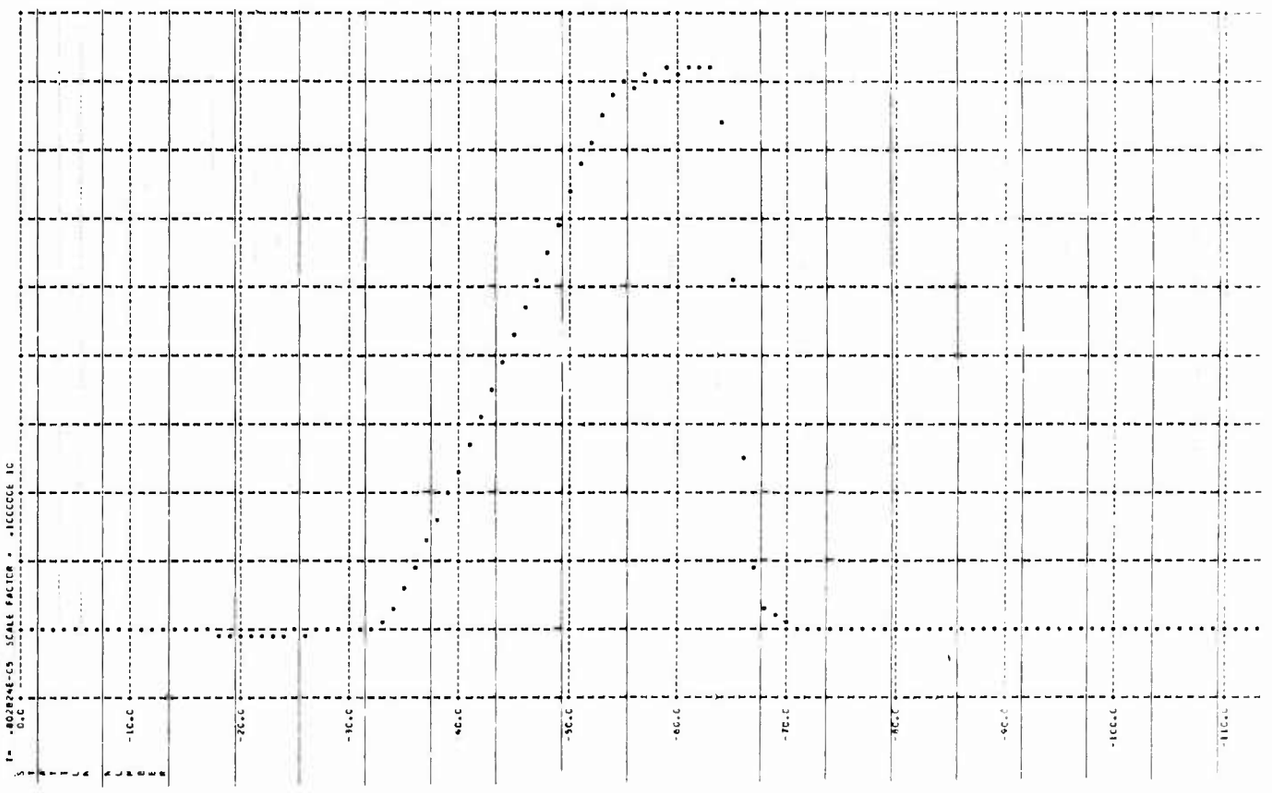

Figure 1 Continued
Stress Profiles at 6 and 8 microseconds

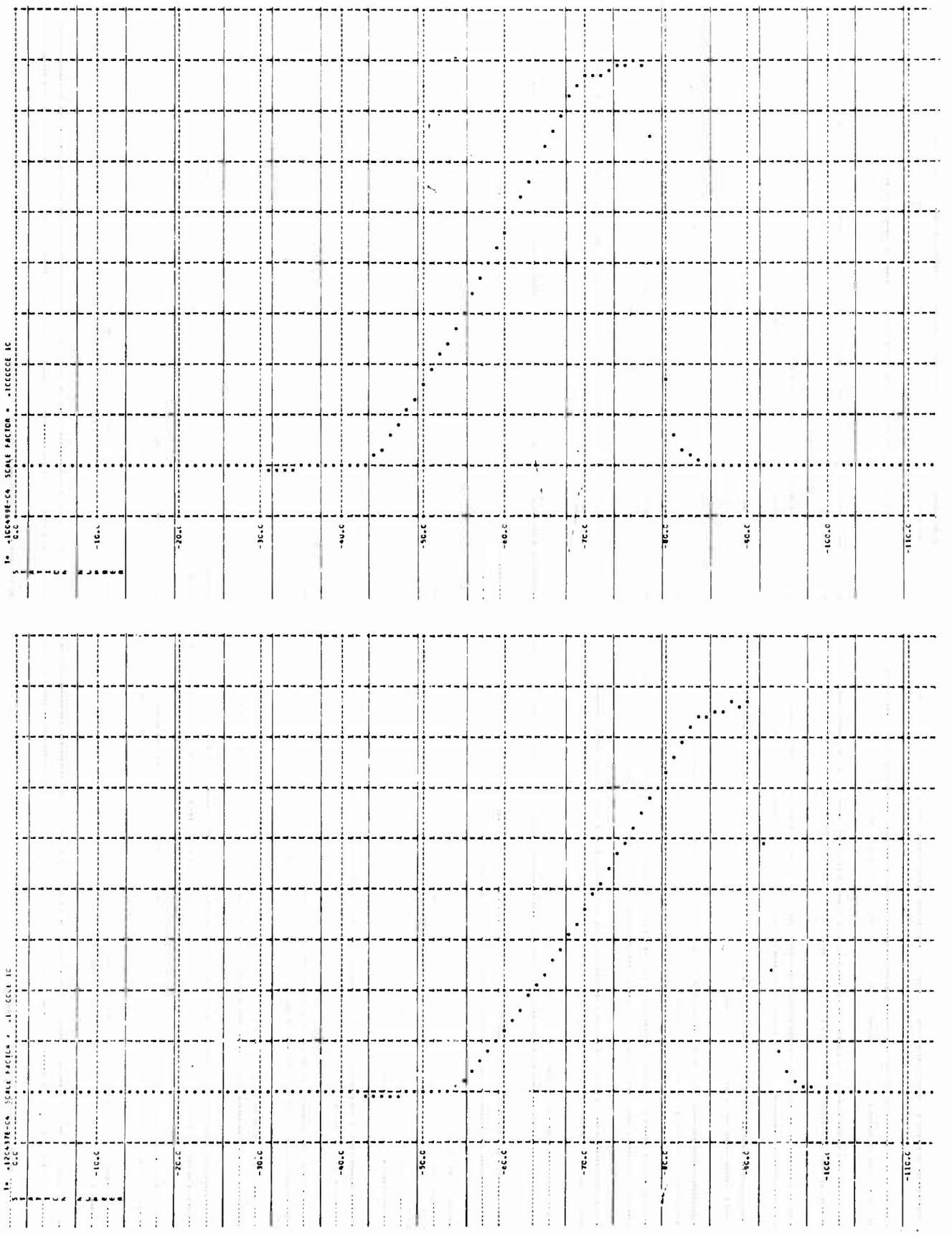

Figure 1 Concluded
Stress Profiles at 10 and 12 microseconds

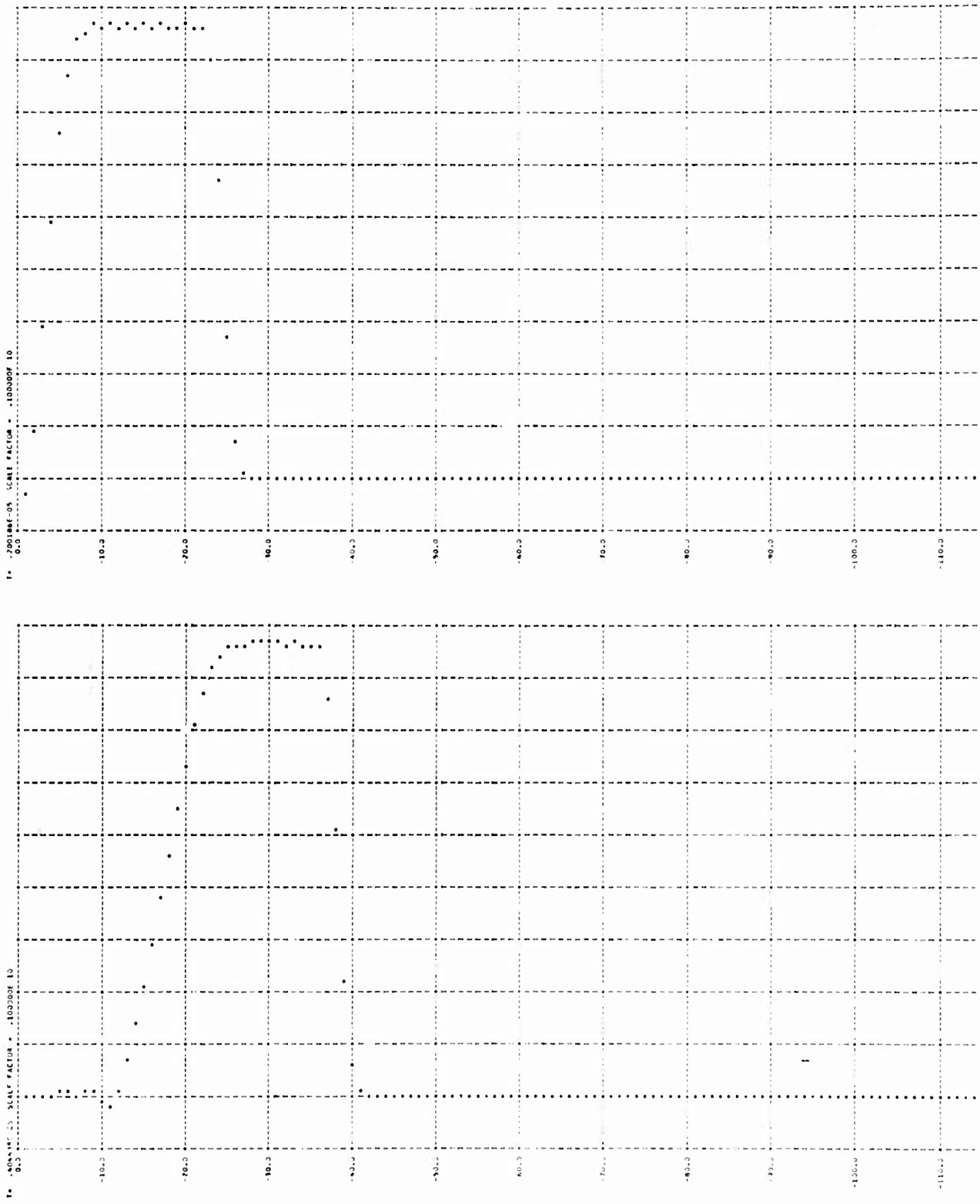

Figure 2. Fluid Plate Impact at Initial Velocity 1.9 km/sec
Stress Profiles at 2 and 4 microseconds

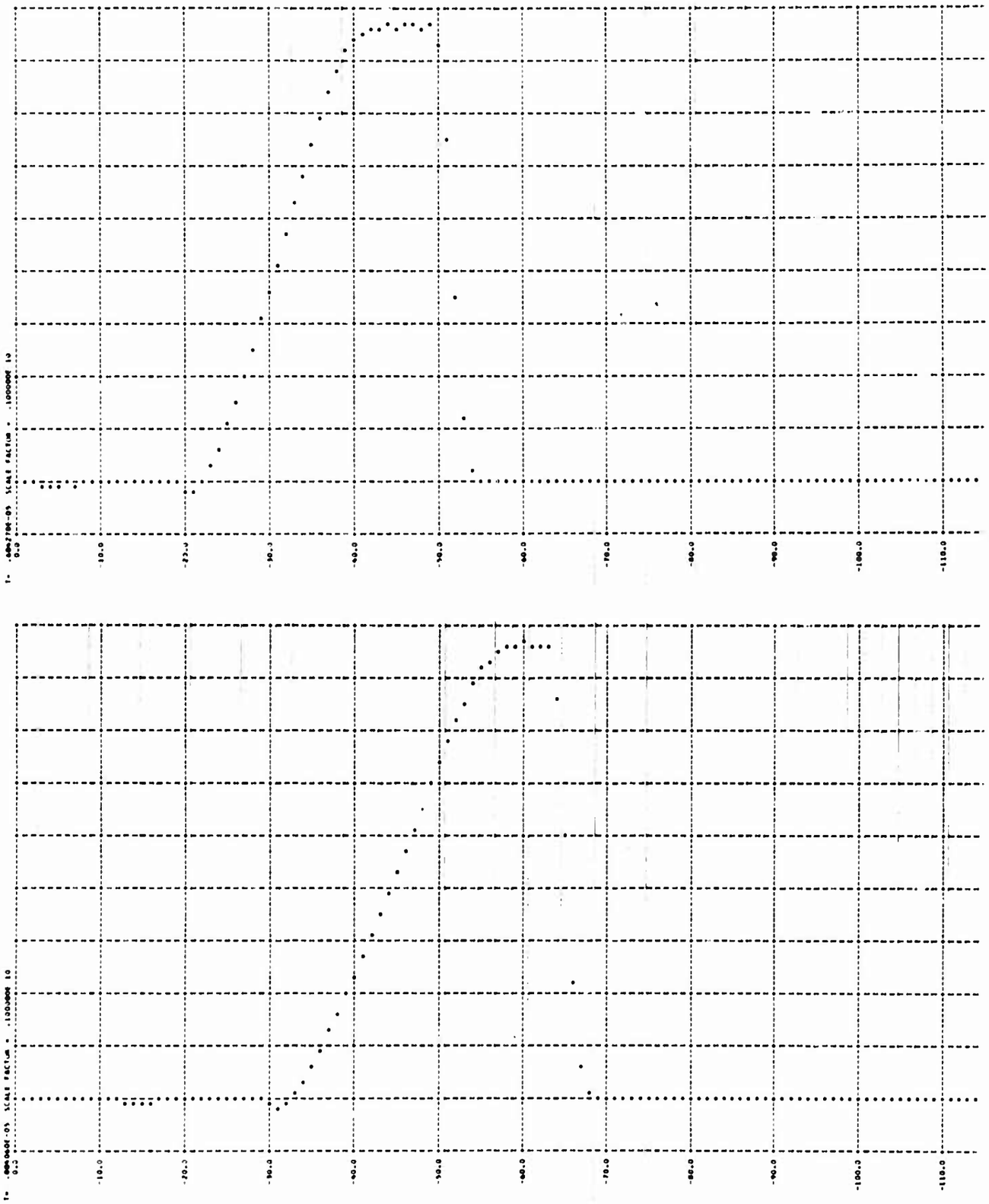

Figure 2 Continued
Stress Profiles at 6 and 8 microseconds

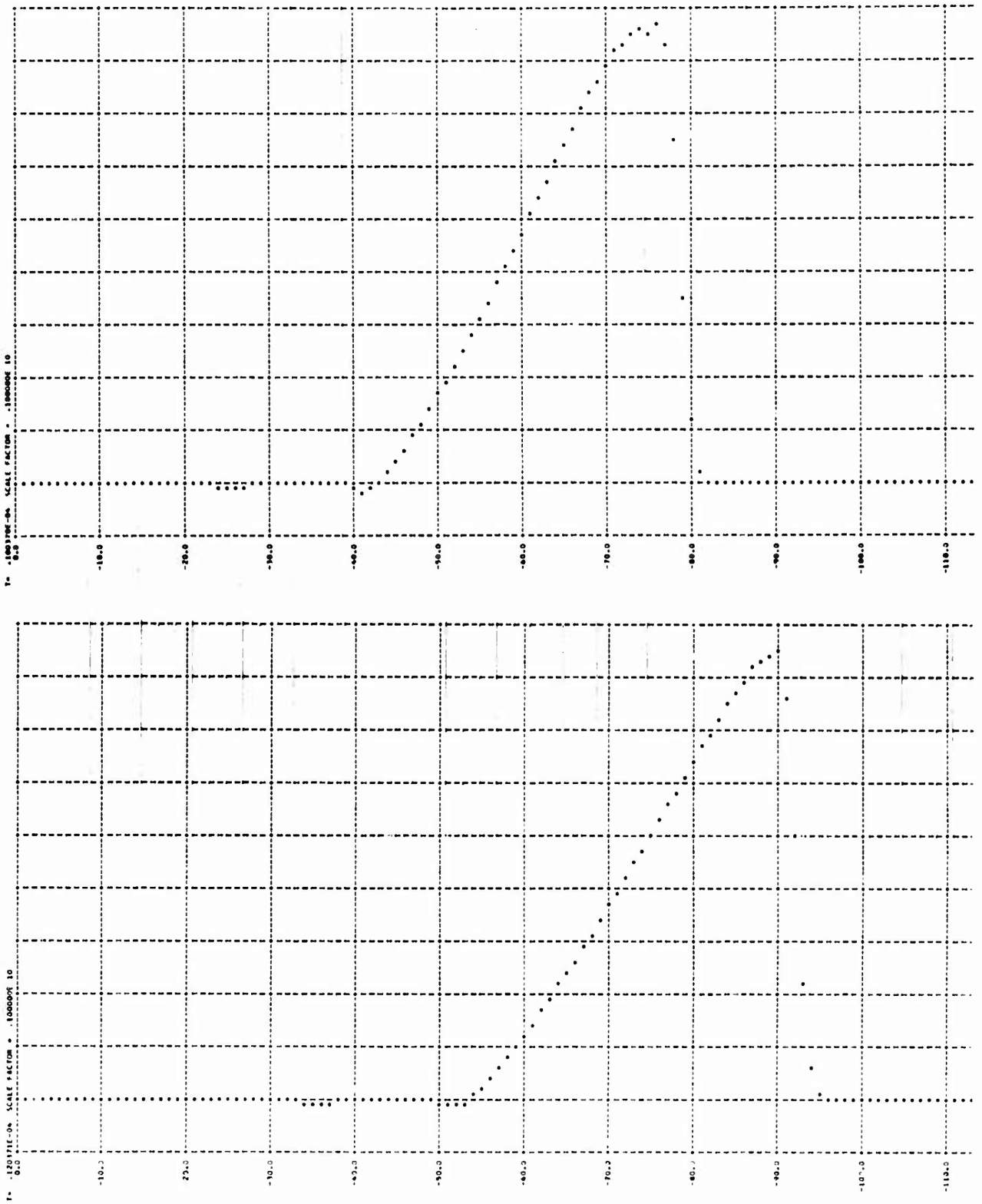

Figure 2 Concluded
Stress Profiles at 10 and 12 microseconds

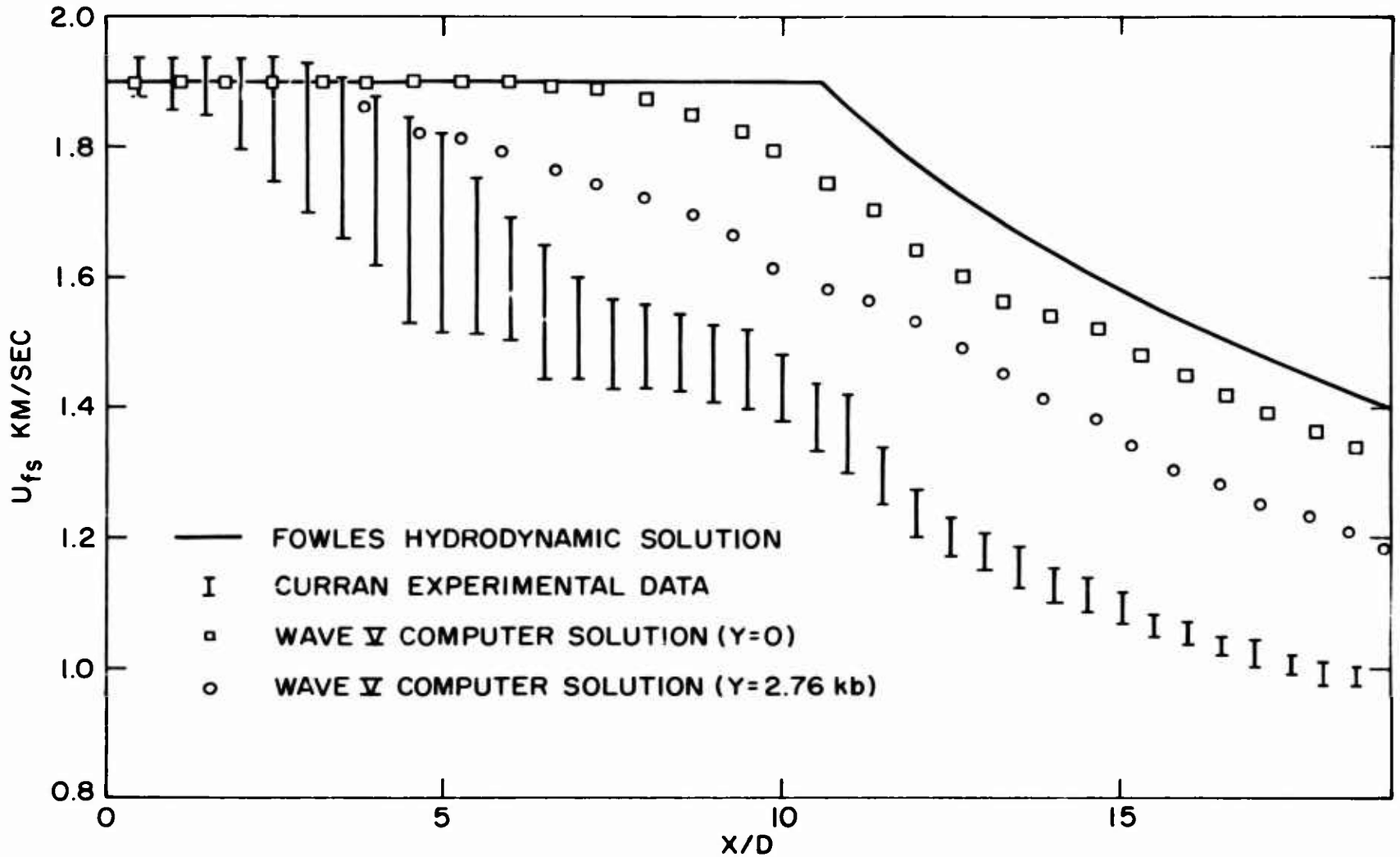

Figure 3. Free Surface Velocity as a Function of Target Plate Thickness in Terms of Driver Plate Thickness for a Driver Plate Velocity of 1.9 km/sec

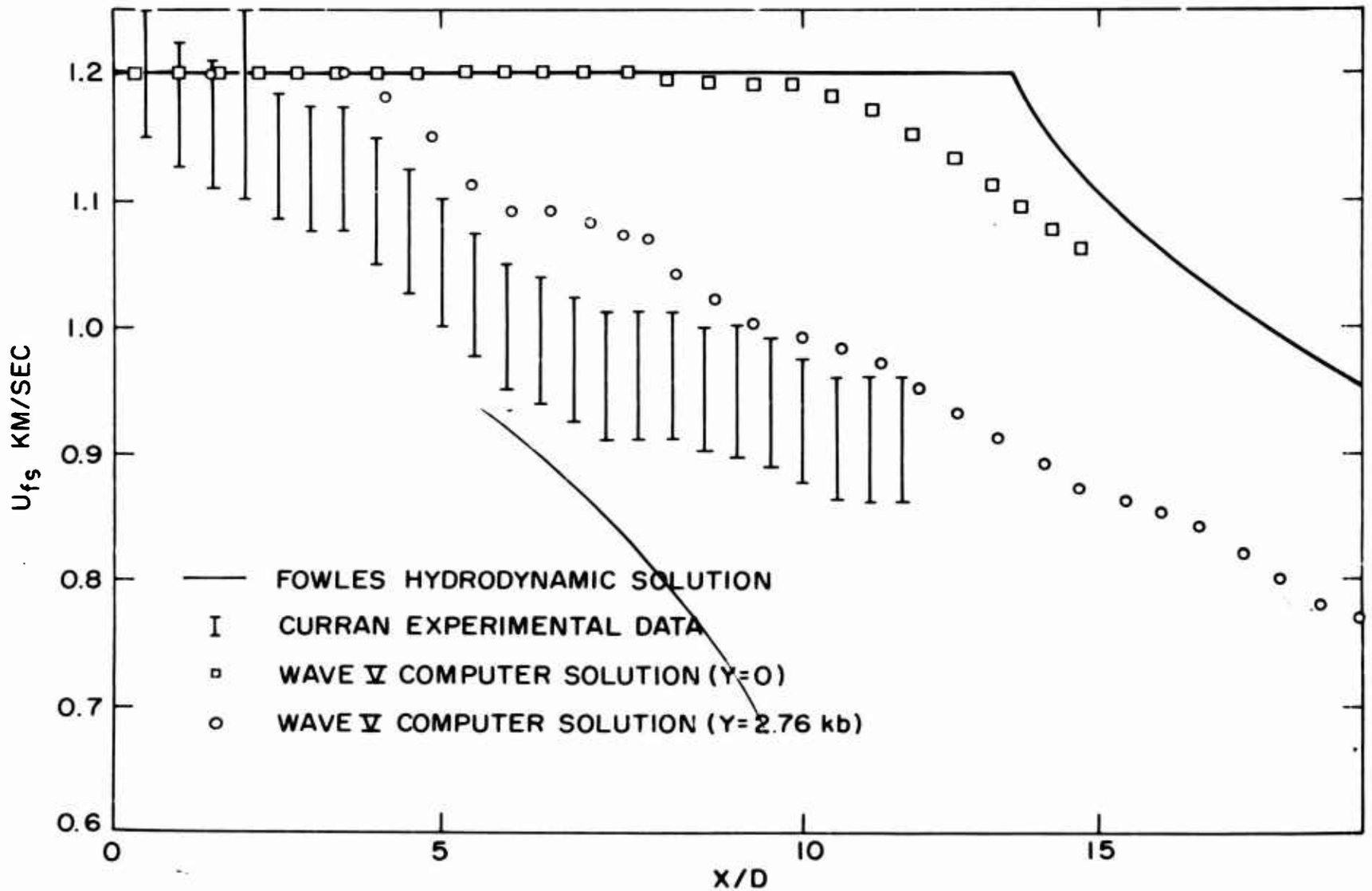

Figure 4. Free Surface Velocity as a Function of Target Plate Thickness in Terms of Driver Plate Thickness for a Driver Plate Velocity of 1.2 km/sec

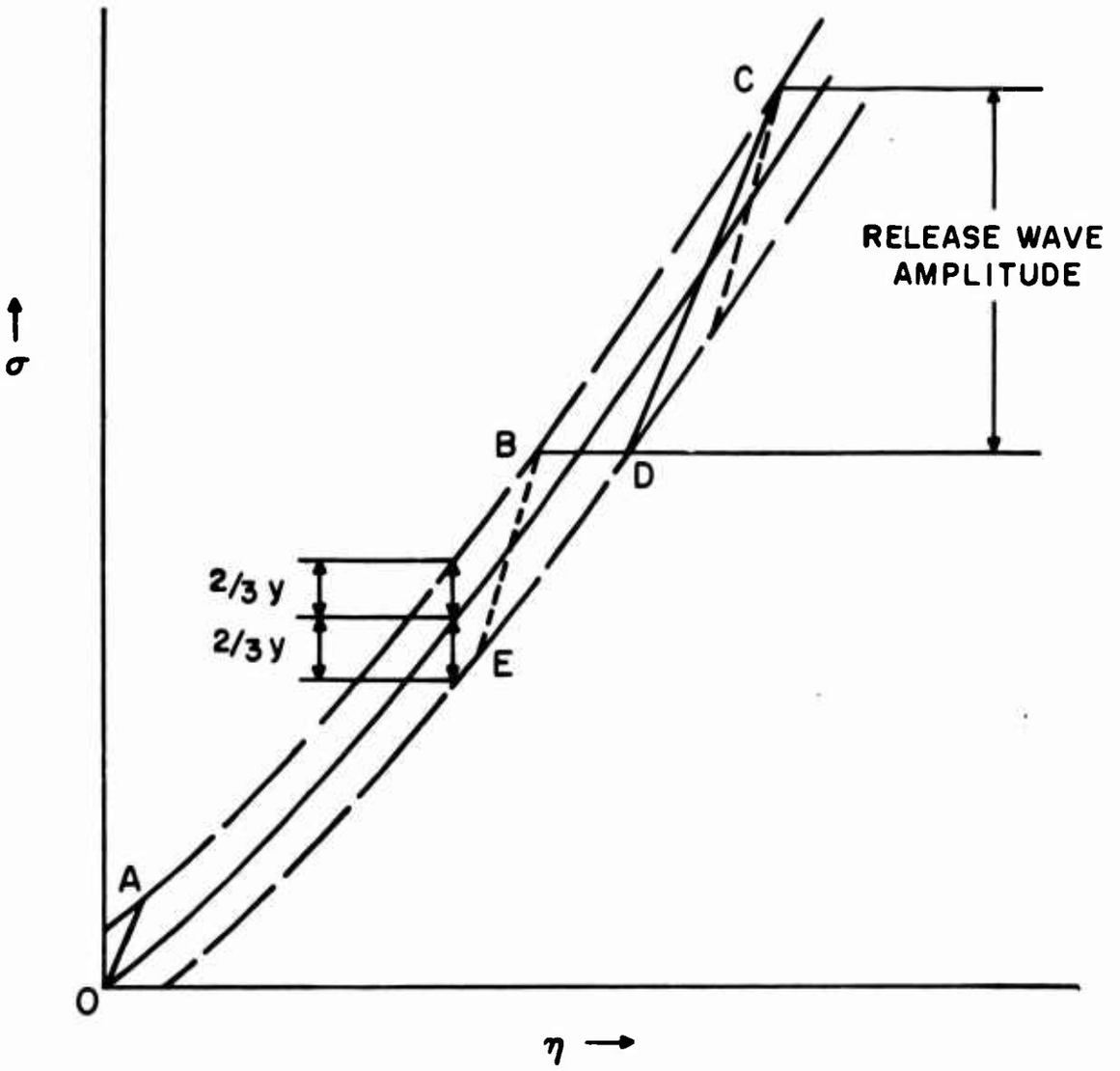

Figure 5. Equation of State Schematic

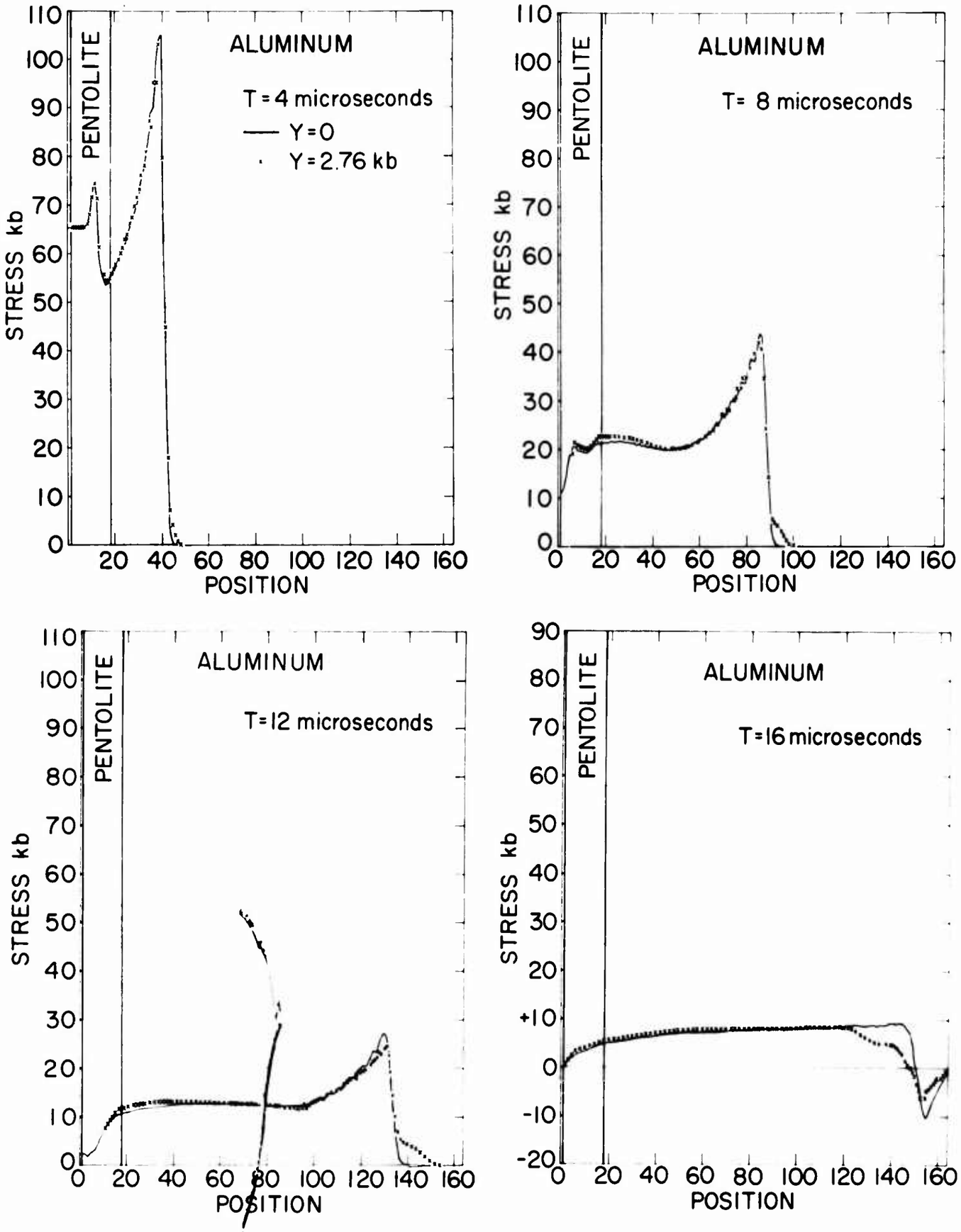

Figure 6. Stress Profiles in an Aluminum Sphere due to a Spherical Cavity Change of Pentolite

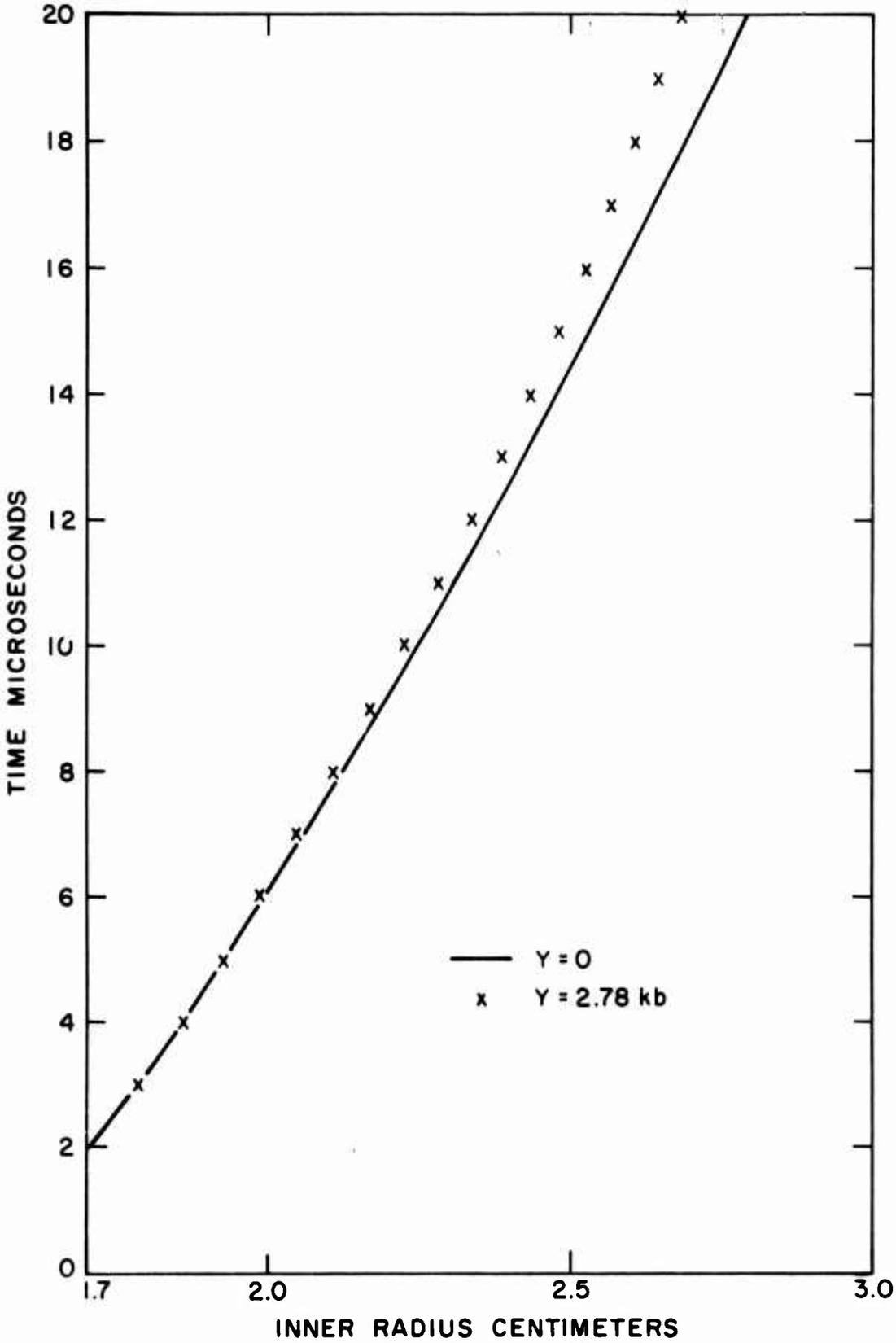

Figure 7. Cavity Radius vs. Time

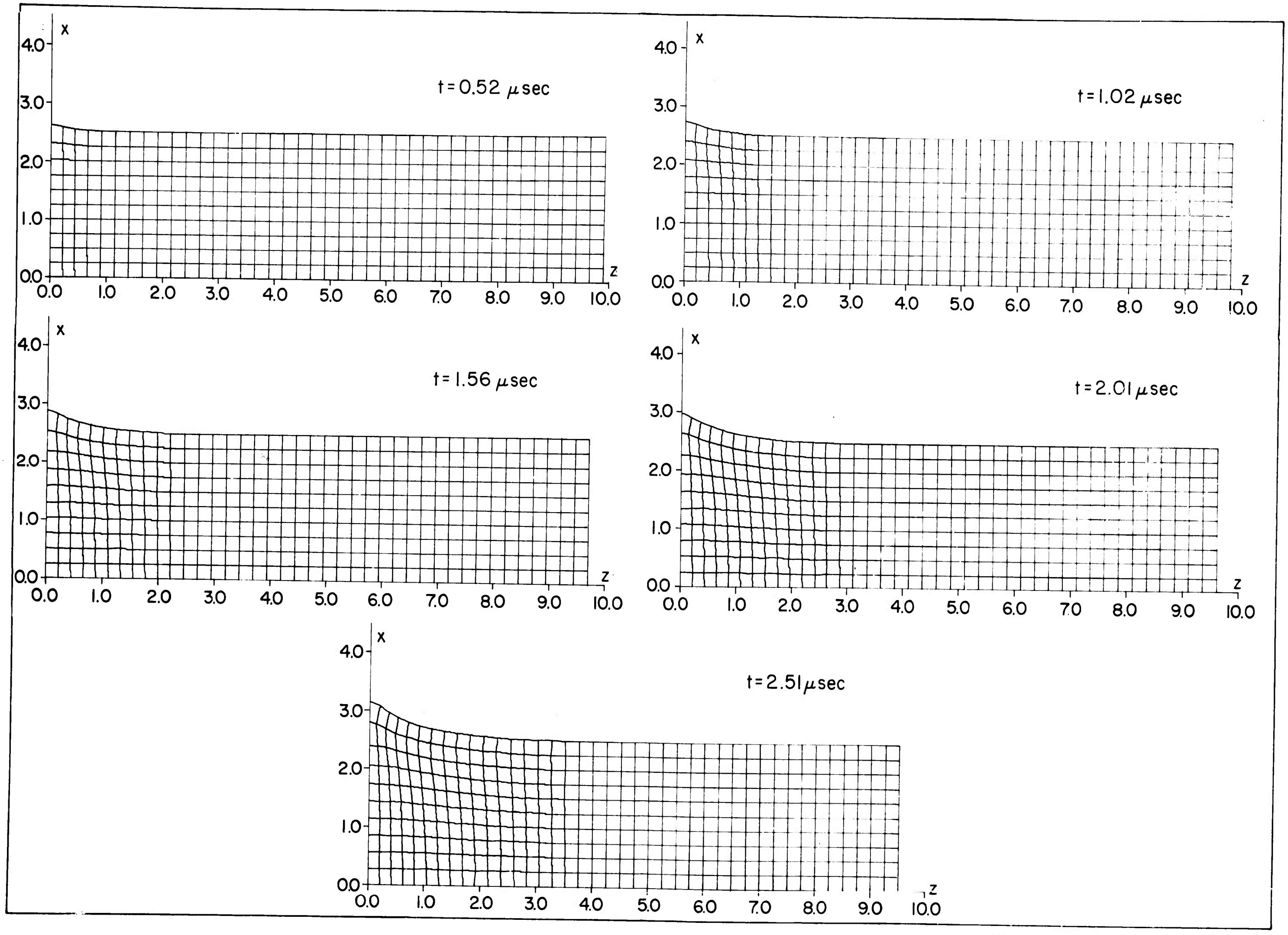

Figure 8. Deformed Mesh Shapes for the Impact of an Aluminum Cylinder on a Smooth Wall

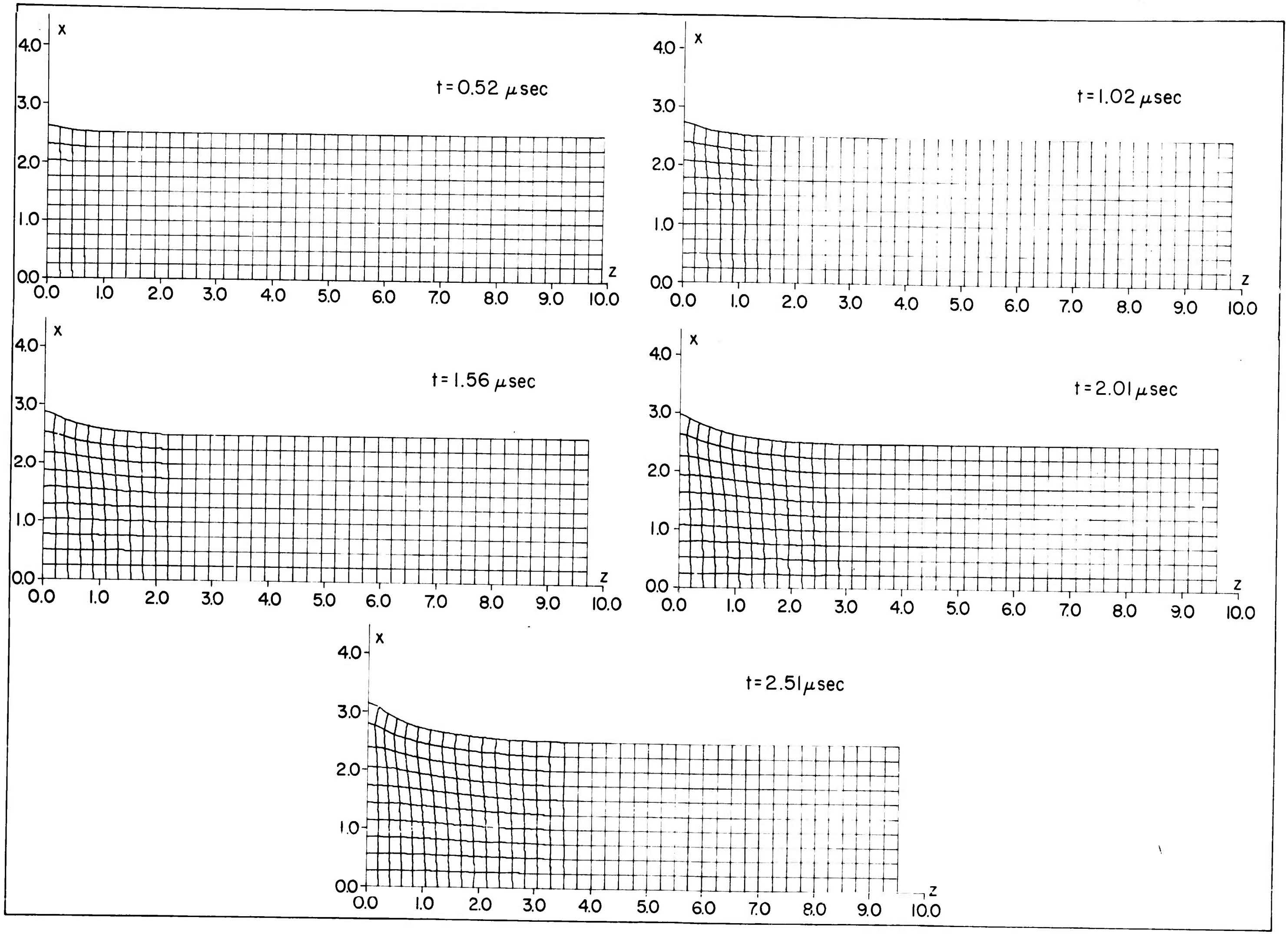

Figure 8. Deformed Mesh Shapes for the Impact of an Aluminum Cylinder on a Smooth Wall

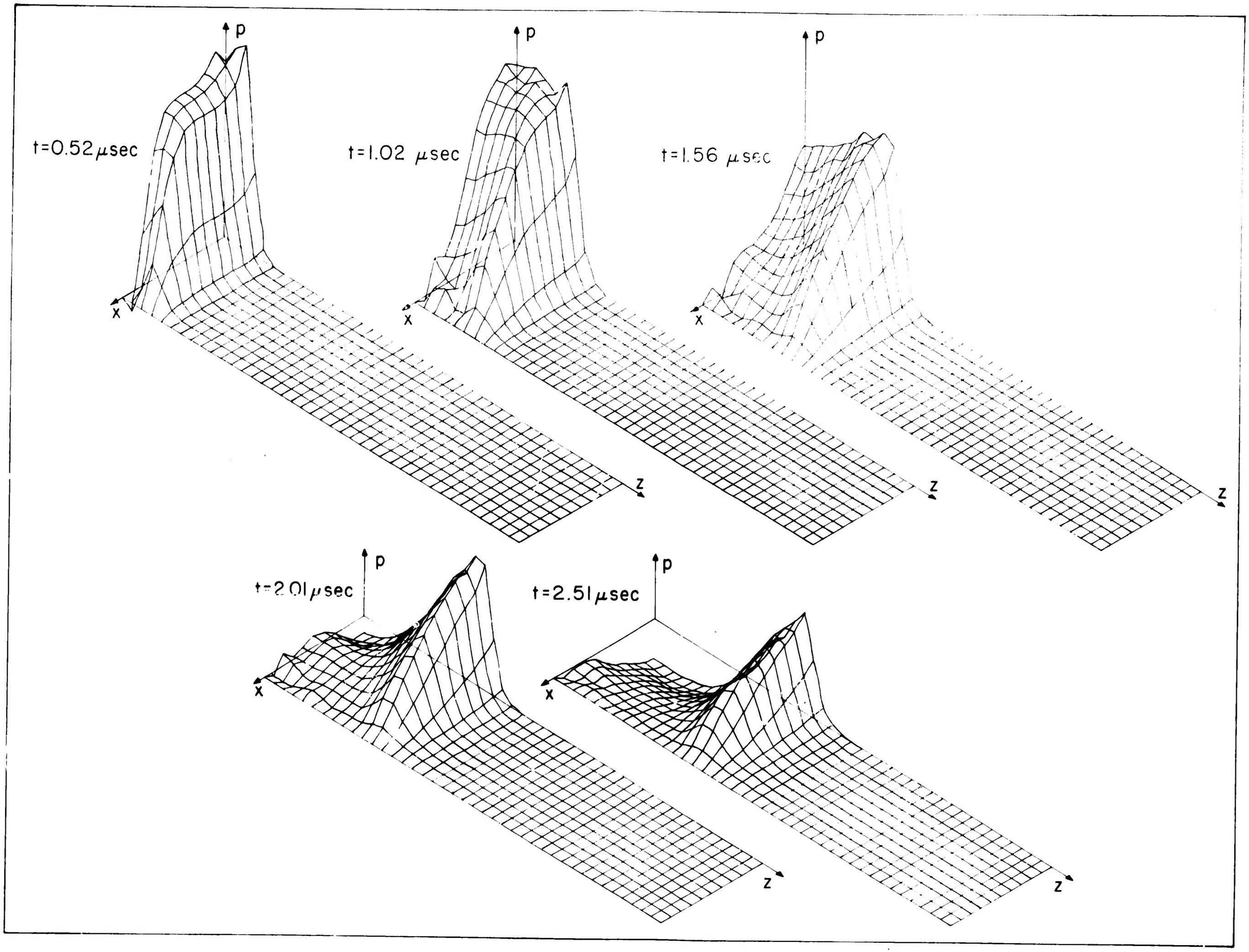

Figure 9. Stress Profiles for the Impact of an Aluminum Cylinder on a Smooth Wall

DISTRIBUTION

No. cys	
	HEADQUARTERS USAF
1	Hq USAF (AFRDP), Wash, DC 20330
1	Hq USAF (AFRNE-B, Maj Dunn), Wash, DC 20330
	MAJOR AIR COMMANDS
	AFSC, Andrews AFB, Wash, DC 20331
1	(SCT)
1	(SCT-2)
1	(SCLT)
	SAC, Offutt AFB, Nebr 68113
1	(OA)
1	(DICC)
1	(DORQM)
1	AUL, Maxwell AFB, Ala 36112
1	USAFIT, Wright-Patterson AFB, Ohio 45433
	AFSC ORGANIZATIONS
1	ASD (SEPIR), Wright-Patterson AFB, Ohio 45433
	RTD, Bolling AFB, Wash, DC 20332
2	(RTN-W, Lt Col Munyon)
1	(RTS)
1	BSD (BSR), Norton AFB, Calif 92409
	KIRTLAND AFB ORGANIZATIONS
1	AFSWC, Kirtland AFB, NM 87117 ATTN: (SWEH)
	AFWL, Kirtland AFB, NM 87117
10	(WLIL)
10	(WLRP, Lt Ward)
1	(WLRM)
1	(WLAV)
	OTHER DOD ACTIVITIES
1	Director, Defense Atomic Support Agency (Document Library Branch), Wash, DC 20301
1	Commander, Field Command, Defense Atomic Support Agency (FCAG3, Special Weapons Publication Distribution), Sandia Base, NM 87115
20	Hq Defense Documentation Center for Scientific and Technical Information (DDC), Bldg 5, Cameron Sta, Alexandria, Va 22314
1	Director, Advanced Research Projects Agency, Department of Defense, The Pentagon, Wash, DC 20301

DISTRIBUTION (cont'd)

No. cys	
2	US Atomic Energy Commission (Headquarters Library, Reports Section), Mail Station G-017, Wash, DC 20545
2	Sandia Corporation (Technical Library), P.O. Box 969, Livermore, Calif 94551
2	Director, Los Alamos Scientific Laboratory (Helen Redman, Report Library), P.O. Box 1663, Los Alamos, NM 87554
2	Oak Ridge National Laboratory (Tech Library), Oak Ridge, Tenn 37831
2	Argonne National Laboratory (Tech Library), 9700 S. Cass Ave., Argonne, Ill 60440
	OTHER
10	Chief, Input Section, Clearinghouse for Federal Scientific and Technical Information, CFSTI, Sills Bldg., 5285 Port Royal Road, Springfield, Va 22151
1	Institute for Defense Analysis, Room 2B257, The Pentagon, Wash 25, DC THRU: ARPA
1	Massachusetts Institute of Technology, Lincoln Laboratory (Document Library), P.O. Box 73, Lexington, Mass 02173
5	Massachusetts Institute of Technology, ATTN: E. A. Witmer, Director Aeroelastic & Structures, Cambridge, Mass 02139
1	General Electric Company - MSD, ATTN: Dr. F. A. Lucy, Room M9505, P.O. Box 8555, Philadelphia 1, Pa
1	Aerospace Corporation, P.O. Box 95085, Los Angeles 45, Calif
2	Stanford Research Institute, ATTN: G-037, External Reports, Menlo Park, Calif 94025
1	Aerospace Corp., ATTN: Mr. Ivan Weeks, Ballistic Missile Div., San Bernardino, Calif
2	AVCO Corporation, Research and Advanced Development Div., ATTN: Chief Librarian, 201 Lowell Street, Wilmington, Mass
2	General Atomic Div, General Dynamics Corp., 10955 John Jay Hopkins Drive, San Diego, Calif 92121
2	Douglas Aircraft Corp., 3000 Ocean Park Blvd., Santa Monica, Calif
2	Lockheed Missiles and Space Co., P.O. Box 504, Sunnyvale, Calif 94088
2	Moleculon Research Corp., 139 Main St., Cambridge 42, Mass
2	E. H. Plesset Associates, Union Bank Bldg., 2444 Wilshire Blvd., Santa Monica, Calif
2	Tech Ops Research, South Avenue, Burlington, Mass
2	Southwestern Research Institute, 8500 Culebra Road, San Antonio, Tex 78206

DISTRIBUTION (cont'd)

No. cys	
2	Republic Aviation Corp., 223 Jericho Turnpike, Mineola, Long Island, NY
2	Ballistic Research Laboratories, Aberdeen, Md
2	National Bureau of Standards, Boulder, Colo
2	Defense Research Laboratories, General Motors Corp., ATTN: A. H. Jones, Santa Barbara, Calif
2	Sandia Corporation, ATTN: W. Herrmann, Division 1124, Sandia Base, NM 87115
2	Drexel Institute of Technology, ATTN: Pei Chi Chou, Philadelphia 4, Pa
2	Department of Aeronautics and Astronautics, Massachusetts Institute of Technology, ATTN: E. A. Witmer, Cambridge 39, Mass
2	Advance Space Technology, Douglas Missile and Space Systems Div., ATTN: J. K. Wall, Santa Monica, Calif
2	Arenberg Ultrasonic Laboratories, Inc., ATTN: D. L. Arenberg, 94 Green Street, Jamaica Plain, Mass
1	Official Record Copy (WLRPX, Lt Ward)

Unclassified
Security Classification

DOCUMENT CONTROL DATA - R&D

(Security classification of title, body of abstract and indexing annotation must be entered when the overall report is classified)

1. ORIGINATING ACTIVITY *(Corporate author)* Massachusetts Institute of Technology Cambridge, Mass	2a. REPORT SECURITY CLASSIFICATION Unclassified 2b. GROUP

3. REPORT TITLE

A LAGRANGIAN FINITE DIFFERENCE METHOD FOR TWO-DIMENSIONAL MOTION INCLUDING MATERIAL STRENGTH

4. DESCRIPTIVE NOTES *(Type of report and inclusive dates)*

Technical Report 30 Sept 62 - 24 June 64

5. AUTHOR(S) *(Last name, first name, initial)*

Herrmann, Walter

6. REPORT DATE November 64	7a. TOTAL NO. OF PAGES 107	7b. NO. OF REFS 19

8a. CONTRACT OR GRANT NO. AF 29(601)-4601 b. PROJECT NO. 5776 c. Task 577601 d. WEB No. 15.018	9a. ORIGINATOR'S REPORT NUMBER(S) WL-TR-64-107 9b. OTHER REPORT NO(S) *(Any other numbers that may be assigned this report)* Contractor's No. 106-2

10. AVAILABILITY/LIMITATION NOTICES

DDC release to OTS is authorized

11. SUPPLEMENTARY NOTES	12. SPONSORING MILITARY ACTIVITY AFWL (WLRPX) Kirtland AFB, NM

13. ABSTRACT

One- and two-space dimensional finite-difference schemes for the Lagrangian numerical solution of problems in the motion of solids, including material strength, are presented. Two dimensional rectangular cartesian or cylindrically symmetric problems may be handled. Results of sample calculations are appended to illustrate the effect of material strength.

DD FORM 1 JAN 64 1473

Unclassified
Security Classification

Unclassified

Security Classification

14. KEY WORDS	LINK A ROLE	LINK A WT	LINK B ROLE	LINK B WT	LINK C ROLE	LINK C WT
Lagrangian method						
Finite difference						
Two-dimensional motion including material strength						
Motion of solids						
Material strength						
Sample calculations methods						

INSTRUCTIONS

1. ORIGINATING ACTIVITY: Enter the name and address of the contractor, subcontractor, grantee, Department of Defense activity or other organization *(corporate author)* issuing the report.

2a. REPORT SECURITY CLASSIFICATION: Enter the overall security classification of the report. Indicate whether "Restricted Data" is included. Marking is to be in accordance with appropriate security regulations.

2b. GROUP: Automatic downgrading is specified in DoD Directive 5200.10 and Armed Forces Industrial Manual. Enter the group number. Also, when applicable, show that optional markings have been used for Group 3 and Group 4 as authorized.

3. REPORT TITLE: Enter the complete report title in all capital letters. Titles in all cases should be unclassified. If a meaningful title cannot be selected without classification, show title classification in all capitals in parenthesis immediately following the title.

4. DESCRIPTIVE NOTES: If appropriate, enter the type of report, e.g., interim, progress, summary, annual, or final. Give the inclusive dates when a specific reporting period is covered.

5. AUTHOR(S): Enter the name(s) of author(s) as shown on or in the report. Enter last name, first name, middle initial. If military, show rank and branch of service. The name of the principal author is an absolute minimum requirement.

6. REPORT DATE: Enter the date of the report as day, month, year; or month, year. If more than one date appears on the report, use date of publication.

7a. TOTAL NUMBER OF PAGES: The total page count should follow normal pagination procedures, i.e., enter the number of pages containing information.

7b. NUMBER OF REFERENCES: Enter the total number of references cited in the report.

8a. CONTRACT OR GRANT NUMBER: If appropriate, enter the applicable number of the contract or grant under which the report was written.

8b, 8c, & 8d. PROJECT NUMBER: Enter the appropriate military department identification, such as project number, subproject number, system numbers, task number, etc.

9a. ORIGINATOR'S REPORT NUMBER(S): Enter the official report number by which the document will be identified and controlled by the originating activity. This number must be unique to this report.

9b. OTHER REPORT NUMBER(S): If the report has been assigned any other report numbers *(either by the originator or by the sponsor)*, also enter this number(s).

10. AVAILABILITY/LIMITATION NOTICES: Enter any limitations on further dissemination of the report, other than those imposed by security classification, using standard statements such as:

(1) "Qualified requesters may obtain copies of this report from DDC."

(2) "Foreign announcement and dissemination of this report by DDC is not authorized."

(3) "U. S. Government agencies may obtain copies of this report directly from DDC. Other qualified DDC users shall request through _____."

(4) "U. S. military agencies may obtain copies of this report directly from DDC. Other qualified users shall request through _____."

(5) "All distribution of this report is controlled. Qualified DDC users shall request through _____."

If the report has been furnished to the Office of Technical Services, Department of Commerce, for sale to the public, indicate this fact and enter the price, if known.

11. SUPPLEMENTARY NOTES: Use for additional explanatory notes.

12. SPONSORING MILITARY ACTIVITY: Enter the name of the departmental project office or laboratory sponsoring *(paying for)* the research and development. Include address.

13. ABSTRACT: Enter an abstract giving a brief and factual summary of the document indicative of the report, even though it may also appear elsewhere in the body of the technical report. If additional space is required, a continuation sheet shall be attached.

It is highly desirable that the abstract of classified reports be unclassified. Each paragraph of the abstract shall end with an indication of the military security classification of the information in the paragraph, represented as *(TS)*, *(S)*, *(C)*, or *(U)*.

There is no limitation on the length of the abstract. However, the suggested length is from 150 to 225 words.

14. KEY WORDS: Key words are technically meaningful terms or short phrases that characterize a report and may be used as index entries for cataloging the report. Key words must be selected so that no security classification is required. Identifiers, such as equipment model designation, trade name, military project code name, geographic location, may be used as key words but will be followed by an indication of technical context. The assignment of links, rules, and weights is optional.

Unclassified

Security Classification